

**T.R.**  
**GEBZE TECHNICAL UNIVERSITY**  
**GRADUATE SCHOOL OF NATURAL AND APPLIED SCIENCES**

**APPLICATION OF PHOTOEMISSION SPECTROSCOPY IN  
SURFACE CHARACTERIZATION OF CHROMIUM OXIDE TO  
DEFINE OXIDE PHASES GROWING BY REACTIVE MAGNETRON  
SPUTTERING DEPOSITION**

**İSMET GELEN**  
**A THESIS SUBMITTED FOR THE DEGREE OF  
MASTER OF SCIENCE  
DEPARTMENT OF PHYSICS**

**GEBZE**  
**2016**

**T.R.**  
**GEBZE TECHNICAL UNIVERSITY**  
**GRADUATE SCHOOL OF NATURAL AND APPLIED SCIENCES**

**APPLICATION OF PHOTOEMISSION  
SPECTROSCOPY IN SURFACE  
CHARACTERIZATION OF CHROMIUM  
OXIDE TO DEFINE OXIDE PHASES  
GROWING BY REACTIVE MAGNETRON  
SPUTTERING DEPOSITION**

**İSMET GELEN**

**A THESIS SUBMITTED FOR THE DEGREE OF  
MASTER OF SCIENCE  
DEPARTMENT OF PHYSICS**

THESIS SUPERVISOR  
ASSOC. PROF. DR. OSMAN ÖZTÜRK  
II. THESIS SUPERVISOR  
ASSOC. PROF. DR. MUSTAFA ERKOVAN

**GEBZE**

**2016**

**T.C.**  
**GEBZE TEKNİK ÜNİVERSİTESİ**  
**FEN BİLİMLERİ ENSTİTÜSÜ**

**FOTOEMİSYON SPEKTROSKOPİSİNİN**  
**REAKTİF MAGNETRON SAÇTIRMA**  
**YÖNTEMİ İLE BÜYÜTÜLEN**  
**OKSİTLENMİŞ KROM FİLMLERİN, OKSİT**  
**FAZLARININ KARAKTERİZASYONUNDA**  
**KULLANILMASI**

**İSMET GELEN**  
**YÜKSEK LİSANS TEZİ**  
**FİZİK ANABİLİM DALI**

**DANIŞMANI**  
**DOÇ. DR. OSMAN ÖZTÜRK**  
**II. DANIŞMANI**  
**DOÇ. DR. MUSTAFA ERKOVAN**

**GEBZE**  
**2016**



## YÜKSEK LİSANS JÜRİ ONAY FORMU

GTÜ Fen Bilimleri Enstitüsü Yönetim Kurulu'nun 15/06/2016 tarih ve 2016/37 sayılı kararıyla oluşturulan jüri tarafından 17/06/2016 tarihinde tez savunma sınavı yapılan İsmet Gelen'in tez çalışması Fizik Anabilim Dalında YÜKSEK LİSANS tezi olarak kabul edilmiştir.

### JÜRİ

ÜYE

(TEZ DANIŞMANI) : Doç. Dr. Osman Öztürk

ÜYE

: Prof. Dr. Savaş Berber

ÜYE

: Yard. Doç. Dr. Furkan Dünder

### ONAY

Gebze Teknik Üniversitesi Fen Bilimleri Enstitüsü Yönetim Kurulu'nun

...../...../..... tarih ve ...../..... sayılı kararı.

İMZA/MÜHÜR

## SUMMARY

The transition half-metal oxides (TMOs) have a wide technological application. Chromium oxide which is a TMOs is performed. The ultra-thin film of these TMOs got a very big attention due to the ultra-thin films could be enhanced in material feature.

The ultra-thin films are prepared in angstrom range by magnetron sputtering. Due to the requirement of the clean environment, the ultra-thin films were prepared under the UHV condition that is obtained by Turbo Mechanical and mechanical pumps. The growth has been employed on the naturally oxidized silicon crystal substrate. The Si crystal is mounted in the system after cleaning. Then the growth has been done by Argon gas which is sputtered the Cr atoms from the target. The scattered Cr atoms accumulate on the crystal. For oxide films, the oxygen was fed to the chamber. The growth has been done by two methods in order to understand the methods of growth effect on the thin film deposition. First, the growth has been initiated with Pulsed DC, then the RF magnetron sputtering has been employed for many ultra-thin films growth for different parameters. The planned variety samples were examined by XPS that is very effective method to analyze the ultra-thin film surface compounds. The thickness was controlled by QCM during growth.

The objective of this work is to grow the  $\text{Cr}_2\text{O}_3$  thin films on Si crystal by magnetron sputtering that are basis for future work of multi-layer specimens that is going to be used for spintronic application as an antiferromagnetic material.

**Key Words: Magnetron Sputtering, Chromium Oxide, XPS, TMOs.**

## ÖZET

Oksite geiş metallerin teknolojik uygulamalarda ok byk bir uygulama alanı vardır. Bundan dolayı bu alıřmada geiş metali olan krom alıřıldı. Kromun bir ka oksitlenmiř fazy vardır. Ayrıca bu alıřmada zerinde durulan ikinci nokta ise ultra ince filmlerle bu alıřmayı gerekleřtirmektir. nk ince filmlerin teknolojik uygulamalarda ok byk avantajları vardır. Bu yzden bu alıřmada angstrom seviyesinde ultra ince filmler hazırlanmıřtır.

Bu alıřmada,  $Cr_2O_3$  ince filmlerin bytlmesi magnetron satırma yntemi ile gerekleřtirilmiřtir. Doęal oksitlenmiř silisyum kristalin zerinde bytlmř olan  $Cr_2O_3$  ultra ince filmler UHV řartlarında bytld. Turbo molekler pump ve dięer pompalar ile yksek vakum elde ediliyor. Argon gazı satırma gazı olarak kullanılmıřtır. Argon gazı saf Cr target'tan (hedef malzeme) Cr atomlarını koparıp alt tařın stnde bymesi saęlanmıř olur.  $Cr_2O_3$  ince filmlerin bymesi iin ortama oksijen belli řartlar altında veriliyor. Bu alıřma da bytme iki yntem ile gerekleřmiřtir. İlk alıřmalar Pulsed DC ile ikinci alıřmalarda ise RF ile ultra ince filmler hazırlanmıřtır. Bu hazırlanmıř ince filmler yzey analizi iin ok etkili bir yntem olan XPS ile analiz edilmiřtir. XPS ultra ince filmin yzeyindeki elementler hakkında bilgi verir. Bytlen ince filmler bytlme sırasında QCM ile kalınlıkları kontrol edilmiřtir.

$Cr_2O_3$  ultra ince filmler yukarda kısaca anlatıldıęı gibi hazırlanmıřtır. Pulsed DC ve RF magnetron satırma yntemleri ile hazırlanmıř numuneler farklı alttař sıcaklıęı ve bazı numuneler bytme iřlemi bittikten sonra tavlama iřlemine tabi tutulmuřtur. Bu farklı parametrelerin etkisi XPS ile incelenmiřtir. Genel olarak hazırlanan rnekler ok katmanlı filmler de antiferromagnetik malzeme olarak spintronik uygulamalarda kullanılabilir.

**Anahtar Kelimeler: Magnetron Satırma, Krom Oksit, XPS, Geiş Metalleri.**

## ACKNOWLEDGEMENTS

I would like to express my deep and sincere gratitude to my supervisor, Assoc. Prof. Dr. Osman Öztürk, who is not only shared his profound scientific knowledge with me but also taught me great lessons of life. His support, suggestions and encouragement gave me the drive and will to complete this work. And I also would like to thank my second supervisor Assoc. Prof. Dr. Mustafa Erkovan since he always encourages me for academic career and he always share his sincere thoughts with me.

I wish to express my deepest thanks to Melek Türksöy Öcal for her support; by sharing her valuable experience, this work becomes possible. I want to thank Asst. Prof. Sibel Tokdemir Öztürk because her valuable advice from my BSc till now. And I also want to thank my colleague Dr. Ali Şems Ahsen, Baha Sakar, Mehmet Emre Aköz for their valuable contribution of knowledge.

It is my privilege to thank my wife Saadet Gelen for her support during writing this thesis. And I am also grateful to my parents, brothers, sisters and aunt for their love and support.

I want to dedicate this work to my little sister Gülcan.

# TABLE of CONTENTS

	<u>Page</u>
SUMMARY	v
ÖZET	vi
ACKNOWLEDGMENTS	vii
TABLE of CONTENTS	viii
LIST of ABBREVIATIONS and ACRONYMS	x
LIST of FIGURES	xiii
LIST of TABLES	xv
1. INTRODUCTION	1
1.1. Half Metal Oxides and Chromium Oxide	3
1.2. Thin Films and Surfaces	8
1.3. Outlines	11
2. EXPERIMENTAL TECHNIQUES	12
2.1. Thin Films Preparations	12
2.1.1. UHV Cluster Chambers	12
2.1.2. Substrate Preparation Before Growth Process	15
2.2. Magnetron Sputtering Thin Film Deposition	16
2.2.1. DC Magnetron Sputtering Process	20
2.2.2. Pulsed DC Magnetron Sputtering Process	21
2.2.3. RF Magnetron Sputtering Process	21
2.3. X-ray Photoelectron Spectroscopy (XPS)	23
2.3.1. Instrumentation for XPS	24
2.3.2. Photoemission Mechanism	26
2.3.3. Surface Sensitivity of Photoemission	31
2.3.4. Experimental Technique	33
2.3.5. Surface Electronic Structure	33
2.3.5.1. Chemical Shifts	34
2.3.5.2. Level Splitting	36
2.3.6. Chemical and Elemental Analysis Composition of Surface	38
2.3.6.1. Quantitative Analysis	38



3. GROWTH OF STABLE FILM OF CHROMIUM OXIDE THIN FILMS	44
3.1. Preparation of Substrate Silicon Single Crystal towards Film Growth by Magnetron Sputtering in UHV condition.	45
3.2. Cr <sub>2</sub> O <sub>3</sub> thin films growth on Si by Pulse D.C Magnetron Sputtering	47
3.3. Cr <sub>2</sub> O <sub>3</sub> thin films growth on Si by RF Magnetron Sputtering	54
3.4. Fitting Process of XPS to Calculate the Cr/O Ratio	60
3.5. Discussion	64
4. CONCLUSION	66
REFERENCES	68
BIOGRAPHY	74
APPENDICES	75

## LIST of ABBREVIATIONS and ACRONYMS

<u>Abbreviations</u>	<u>Explanations</u>
<u>and Acronyms</u>	
$\text{\AA}$	: Angstrom
$E_B$	: Binding Energy
$E_f$	: Fermi Level
$E_k$	: Electron Kinetic Energy
$E_v$	: Vacuum Level
$E_x$	: Excitation Energy
$E_k^{Auger}$	: Auger Electron Energy
$\Phi_s$	: Sample Work Function
$\Phi_{spec}$	: Spectrometer Work Function
$\lambda$	: Full Width Half Maximum
$\lambda_a$	: Attenuation Length of Electrons
2D	: Two Dimension
AES	: Auger Electron Spectroscopy
AFM	: Antiferromagnetic
Ag	: Silver
Al	: Aluminum
Ar	: Argon
$Ar^+$	: Argon Ion
ASF	: Atomic Sensitivity Factor
Au	: Gold
BE	: Binding Energy
cm	: Centimeter
Co	: Cobalt
Cr	: Chromium
Cu	: Copper
CVD	: Chemical Vapor Deposition
DC	: Direct Current
E	: Energy

eV	: Electron Volt
Fe	: Iron
FWHM	: Full Width Half Maximum
GTU	: Gebze Technical University
h	: Planck Constant
HCP	: Hexagonal Close Packed
HSA	: Hemispherical Analyzer
HV	: High Vacuum
I	: Intensity
IMFP	: Inelastic Mean Free Path
KE	: Kinetic Energy
LEED	: Low Energy Electron Diffraction
m	: Meter
MBE	: Molecular Beam Epitaxy
MFC	: Mass Flow Controller
Mg	: Magnesium
min	: Minute(s)
Mn	: Mangan
MS	: Magnetron Sputtering
MSD	: Magnetron Sputter Deposition
nm	: Nanometer
O	: Oxygen
PBN	: Pyrolytic Boron Nitride
Pt	: Platinum
Pulsed DC	: Pulsed Direct Current
PVD	: Physical Vapor Deposition
QCM	: Quartz Crystal Microbalance
RF	: Radio Frequency
RGA	: Residual Gas Analyzer
RSF	: Relative Sensitivity Factor
RT	: Room Temperature
s	: Second
sccm	: Standard Cubic Centimeter per Minute

Si	:	Silicon
srvy	:	Survey
Ti	:	Titanium
TMOs	:	Transition Metal Oxides
TMP	:	Turbomolecular Pump
TSP	:	Titanium Sublimation Pump
UHV	:	Ultra High Vacuum
W	:	Watt
XPS	:	X-Ray Photoelectron Spectroscopy
$\nu$	:	Frequency



## LIST of FIGURES

<b><u>Figure No:</u></b>	<b><u>Page</u></b>
2.1: Magnetron sputtering and XPS analytic chamber.	13
2.2: The schematic view of Turbomolecular (TMP) and Rotary Pumps are combined by Foreline.	14
2.3: The schematic view of Magnetron Sputtering Chamber: RF, DC, and Pulsed DC sources. Vacuum Pump and Load Lock.	20
2.4: Magnetron Sputtering Plasma and Coating Process.	22
2.5: X-ray Photoelectron Spectrometer Analytic Chamber.	26
2.6: a) Photoelectron effect and b) Auger process.	27
2.7: X-ray source, twin anode (Al, Mg).	28
2.8: Characteristic & Bremsstrahlung radiation.	29
2.9: Energy level schematic for XPS binding energy measurements.	30
2.10: The mean free path of electrons in different solids as a function of electrons kinetic energy.	32
2.11: Chemical shift of C1s for different chemical bonding.	36
2.12: The exchange splitting of a) Fe2p, b) Mn2p for YFMO and c) Cr2p, d) Mn2p for YCMO.	37
2.13: The shake-up satellite peak of the Cu.	40
2.14: Plasmon loss features from clean Aluminum.	41
2.15: Curve fits to the Fe2p region of the reference sample after applying three different background subtraction methods.	42
2.16: Comparison of a Gaussian and a Lorentzian function with FWHM = 2 eV with the result of the convolution of both, the Voigt function.	43
3.1: Specimen and sample holder	46
3.2: The spectrum of Cr growth on naturally oxidized silicon crystal (100).	48
3.3: The growth of Cr <sub>2</sub> O <sub>3</sub> is performed under 0.3 sccm Argon gas and for 0.2, 0.23, 0.3 sccm Oxygen gas XPS spectrum.	49
3.4: The XPS of RT substrate growth of Cr <sub>2</sub> O <sub>3</sub> and the sample was annealed from RT to 300°C.	51

3.5:	The XPS result of Cr <sub>2</sub> O <sub>3</sub> growth at 20 W and substrate 250°C and then the sample was employed post annealing at 400°C.	53
3.6:	The growth of Cr <sub>2</sub> O <sub>3</sub> at 400°C substrate and 20 W, MFC of oxygen is 0.23 sccm and argon is 3 sccm.	54
3.7:	The XPS spectrum of 3 sccm Argon, 0.23 sccm Oxygen, 121 Å, substrate temperature is 400°C and post annealing has been done for 15 minutes at 400°C two times and then after one day it again annealed at 500°C for 15 minutes for the RF1 specimen.	56
3.8:	The growth of the RF2 sample has been done for 3 sccm Argon, 0.23 sccm Oxygen, 121 Å, substrate temperature is 400°C and post annealing has been done for 20 minutes at 500°C.	57
3.9:	The growth has been done under 3 sccm Argon, 0.23 sccm Oxygen, 121 Å, substrate temperature is 400°C and post annealing has been done for 15 minutes at 500°C, XPS spectrum of the RF3 specimen.	58
3.10:	The growth of RF4 specimen has been done for 3 sccm Argon, 0.23 sccm Oxygen, 177 Å, substrate temperature is 400°C and post annealing has been done for 15 minutes at 400°C, XPS spectrum of a) Cr 2p and b) O 1s.	59
3.11:	The growth has been done for 3 sccm Argon, 0.23 sccm Oxygen, 180 Å, substrate temperature is 400°C and post annealing has been done for 15 minutes at 400°C, XPS spectrum of RF5 specimen.	59
3.12:	The survey spectrum of Cr-Oxide surfaces and natural oxidized Si (100) crystal.	62
3.13:	Fitting process of a) Cr2p and b) O1s.	63

## LIST of TABLES

<b><u>Table No:</u></b>	<b><u>Page</u></b>
3.1: The Cr growth on Si crystal with Pulsed DC Magnetron Sputtering in UHV condition at RT for 3 sccm Argon pressure and for 0.23 and 0.3 sccm oxygen pressure Cr phases peaks.	50
3.2: The XPS of RT substrate growth of Cr on Si crystal and the sample was annealed for RT to 300°C.	52
3.3: The Photoemission peak shifts of Cr 2p <sub>3/2</sub> are shown for different Cr-Oxide formation.	60
3.4: The calculation of the four samples Cr/O ratios.	64

# 1. INTRODUCTION

The antiferromagnetic (AFM) material has gotten big attention in recent years due their spintronic application. The antiferromagnetic materials show that the magnetic moments of atoms or molecules are related to the spins of electrons. The spins are pointing in opposite direction with their neighboring spins. The antiferromagnetic property generally exists among the transition metal. Mostly, transition metal oxide materials have that feature. The AFM can be used in spintronic application. The spintronic application is going to be used in data storage, sensors and etc. In this work, the  $\text{Cr}_2\text{O}_3$  has been chosen to study, due to its antiferromagnetic feature that can be used in spintronic application. One of the other important study is in this work is that the growth has been done on natural oxidized silicon crystal substrate as thin film which has an angstrom range thickness. Another reason is that chromium is one of the transition metal that has very strong magnetic moment. That can be improved by ultra-thin films, and it can be used for the multilayer thin film. Cr oxides have several phases, such as  $\text{CrO}$ ,  $\text{CrO}_2$ ,  $\text{Cr}_2\text{O}_3$  and  $\text{Cr}_3\text{O}_4$ .  $\text{CrO}_2$  is one of the chromium oxide that is believed to be a half metallic ferromagnetic with a metallic band structure for one spin and an insulating band structure for the other [1]-[3]. Its ferromagnetic property makes it significant for spintronic application. Due to the merit of  $\text{CrO}_2$ , it is used in some area such as corrosion resistance and high coercivity so it is used in magnetic recording media and it can be used in spin-valve devices for magnetic field sensing and information storage [2]. On the other hand, surface features of  $\text{CrO}_2$  can be degraded in  $\text{Cr}_2\text{O}_3$  phase [4] because of the environmental interruption. For instance, the  $\text{CrO}_2$  easily gets effect from the temperature. If the temperature is above about  $280^\circ\text{C}$ ,  $\text{CrO}_2$  decomposes to the most stable oxide of chromium,  $\alpha\text{-Cr}_2\text{O}_3$  and  $\gamma\text{-Cr}_2\text{O}_3$  has the corundum structure, it is used a very wide, for instance, it is an important polymerization catalyst, and it is used in passivating stainless steel [5]. It is also known that  $\text{Cr}_2\text{O}_3$  films have been deposited by sputtering and, chemical vapor deposition (CVD) and plasma spray pyrolysis. Previous studies report a good wear resistance and a low coefficient of friction but hardness values well below the bulk value. Furthermore, such as higher than  $1600^\circ\text{C}$  the stable oxide of chromium is a tetragonally distorted  $\text{Cr}_3\text{O}_4$  spinel phase [6]. The formation of  $\gamma\text{-Cr}_2\text{O}_3$ , a cubic spinel phase, has also been reported for certain thin film growth conditions. Ordered single-



crystal samples of any of these chromium oxides are unavailable making their thin films preparation more crucial. In addition to all above comments, currently chromium oxide thin inter layers are studied in some researches about the multilayer thin films towards the variety of technological applications. Such as  $\text{Cr}_2\text{O}_3$  can be used as an AFM for multilayer thin films [7], [8]. That's why my thesis is about developing ultra-thin layer of chromium oxides in well controlled manner.

The significant part is that researches were focused on the half metallic-metal oxides films and the device components on the basis of these material. To develop such advanced technological materials in multi-layer films form contains many challenging steps due to the complexity. Another challenge is that to fabricate them with long stability since  $\text{CrO}_2$  cannot stay long to maintain its phase. However,  $\text{Cr}_2\text{O}_3$  could keep its structure. The new interesting materials with improved properties are essential subject for the researches among science and technology to bind advanced devices and multifunctional materials. It brings that producing deep knowledge of properties of the materials on the atomic scale is necessary in order to understand the origin of their macroscopic behavior. In condensed matter, nano-systems and transition-metal oxides are expected to lead to a whole new range of electronic devices based on spin transport. The new materials built by nano-structures with new tunable properties require a precise knowledge of the structure. As long as the scale is reduced in researches, the knowledge of valance band and surface electronic structure becomes more dominant to find out mechanism in the nanometer range. As chromium oxide thin films have wide applications area from the hardness values and low friction of surfaces to the device based on multi-layer magnetic materials, it has many oxide phases like  $\alpha\text{-Cr}_2\text{O}_3$ ,  $\gamma\text{-Cr}_2\text{O}_3$ ,  $\text{CrO}_2$ ,  $\text{CrO}_3$ ,  $\text{Cr}_8\text{O}_{21}$ ,  $\text{Cr}_2\text{O}_5$ , and,  $\text{Cr}_3\text{O}_4$ ; that's why it is very critical to understand the relationship between the fabrications and the properties.

In literature, the chromium oxide films have been growth by Chemical Vapor Deposition (CVD) [9], Plasma Spray Pyrolysis, Molecular Beam Epitaxy (MBE) [10], [11], [12], Sputter [13] and Pulsed Laser Deposition (PLD) [13], [14]. In our study the chromium oxide films will be grown in UHV ( $10^{-8}$  and  $10^{-10}$  mbar) conditions by using Magnetron Sputtering Depositions during the growth the vacuum pressure is around  $10^{-3}$  mbar. The thickness of films on naturally Oxide Si Substrates vary in range of 20 Å to 200 Å. In order to define oxide phase, the photoemission analytical technique, XPS, will be used. This helps to characterize the electronic properties and chemical stoichiometry of the growth surfaces.

## 1.1. Half Metal Oxides and Chromium Oxides

The transition metal oxides (TMOs) become very popular in past decades. This is due to the main materials for the state of the art technology product. Metal oxides are a crucial class of chemicals having wide-range applications in many areas of chemistry, physics and material science. Transition metal oxides have received considerable attention in recent years by the reasons of their catalytic, electronic and magnetic properties. Furthermore, they are very significant for semiconductor, passivation, and magnetic material devices. And they are fabricated for micro-electronic circuits, sensors, fuel cells, and as catalyst. With nanoscale metal oxides are expected to possess better properties than those of bulk metal oxides. Metal oxide thin films have nano-size and high density of cover edge surface sites; herewith, they can demonstrate unique physical-chemical properties.

In addition, for exemplifying the TMOs;  $\text{Fe}_x\text{O}_y$ ,  $\text{Co}_x\text{O}_y$ ,  $\text{Cr}_x\text{O}_y$  are more common metal oxide materials that are being considered in science research. Hence, the main goal is to obtain  $\text{Cr}_2\text{O}_3$  phase due to the many merit of it. There are some parameters that are considered because of their significant effect on growth of  $\text{Cr}_2\text{O}_3$  phases. One of the crucial parameter is the growth methods; there are many steps for the preparation of transition metal oxide thin films; in this work, two methods have been employed, and they are going to be explained. Each method has its own specific parameters for growth. In this study, to be able to get a very well ultra-thin films of chromium oxide, have obtained by two growth methods which were Pulsed DC and RF magnetron sputtering.

$\text{CrO}_2$  is one of the chromium oxide phases that has many applications. Besides of that it also has taken part in growth of  $\text{Cr}_2\text{O}_3$  phase, because as already aforementioned the  $\text{CrO}_2$  decomposed to the  $\text{Cr}_2\text{O}_3$  such as when  $\text{CrO}_2$  thin films heat to around  $300^\circ\text{C}$ , it decomposes.  $\text{CrO}_2$  is one of the transition metal oxides that have a rutile structure, due to its valance region, it has spin polarization that shows semi-metal feature and ferromagnetic feature, its near region fermi level has spin polarization that it almost has 100 % spin polarization [1], [6]. Due to this feature, it can be used in magnetic field sensor and records. As a result of this, it is a promising material for magnetic applications. Moreover, it can be used for magnetic tunnel junctions, and it also can be used to develop the spin valves for spintronic devices [16]. According to

the study, under 1atm oxygen pressure, between 23°C and 390°C, CrO<sub>2</sub> surfaces thermodynamically are stable and it has more organized structure [2]. On the other hand, it shows quasi-steady feature for the other conditions. Due to its quasi-steady it can be transfer to the Cr<sub>2</sub>O<sub>3</sub> form which is more stable form of the chromium phases by change the oxygen pressure and temperature. Mostly, chromium oxide thin films are transferred to the corundum-Cr<sub>2</sub>O<sub>3</sub> form which is more stable phase through chromium oxides phases. The transformation depends on thickness, growth temperature, and ambient oxygen pressure. In the forward pages, it is going to be explained deeply with many performed parameters, for instance, when the sample annealing to around 300°C, the thin film shows strongly Cr<sup>3+</sup>. In vacuum condition, CrO<sub>2</sub> surface, without care about the temperature and thickness just losing oxygen then it becomes Cr<sub>2</sub>O<sub>3</sub>. It is not easy to attain CrO<sub>2</sub> phase; due to the difficulty of growth of CrO<sub>2</sub> thin films. And its stability is also a big issue. Cr<sub>2</sub>O<sub>3</sub>, however, is more stable and can be grown easily rather than CrO<sub>2</sub>. Due to the previous statements, the aim of this study is growing the Cr<sub>2</sub>O<sub>3</sub> ultra-thin films with reactive magnetron sputtering on naturally oxide silicon single crystal. In this work, reactive magnetron sputtering is preferred because, it is suitable for industrial application and possible to grow a very well ultra-thin films. The magnetron sputtering is performed in UHV condition that has base pressure less than 10<sup>-9</sup> mbar. It provides controlled growth of Cr<sub>2</sub>O<sub>3</sub> thin films thin films. Chromium transition metal has different oxide phases such as CrO<sub>3</sub>, Cr<sub>2</sub>O<sub>3</sub>, Cr<sub>8</sub>O<sub>21</sub>, Cr<sub>2</sub>O<sub>5</sub>, CrO<sub>2</sub>, and Cr<sub>3</sub>O<sub>4</sub>. CrO<sub>2</sub> and Cr<sub>2</sub>O<sub>3</sub> which are the most preferred for studies. In this work, some phases have been seen in the films growth of chromium oxide. Even though the Cr<sub>2</sub>O<sub>3</sub> was the goal, the other phases can be seen from the XPS spectrum. But after some treatment, the single Cr<sub>2</sub>O<sub>3</sub> phase can be obtained, and it is going to be illustrated in the later parts. Specifically, the Cr<sub>2</sub>O<sub>3</sub> has been sought because of its stability through all Cr<sub>x</sub>O<sub>y</sub> phases thermodynamically, and also this phase is insulator [3], [5], [15] and this phase also displays antiferromagnetic feature [17]. Due to its hardest and resistance to chemical, it has been used in many applications in literature [18]-[23]. One of the application is piezomagnetism in epitaxial Cr<sub>2</sub>O<sub>3</sub> thin films and spintronic application [16].

CrO<sub>2</sub> has a quasi-steady property and this feature is a handicap. Therefore, the thin film of CrO<sub>2</sub> can be transformed to Cr<sub>2</sub>O<sub>3</sub> phase which has antiferromagnetic and insulator feature by changing the temperature, and it is thermodynamically more stable [10], [24]. At the same time under the atmospheric condition it can be transferred to

the Cr<sub>2</sub>O<sub>3</sub> phase [25]. Due to unwanted restriction growth of CrO<sub>2</sub> and unstable of this phase, CrO<sub>2</sub> based technological applications majorly are restricted. In general, there are two main restrictions to use CrO<sub>2</sub> in technological application. One of the problems is the obtaining of pure CrO<sub>2</sub> phase or multiple structures due to the growth difficulty and under atmospheric instability. The growth of CrO<sub>2</sub> films and multiple layer preparation are preferred under low pressure ( $\leq 1$  bar) rather than using high pressure. However, Shibasaki Y et al., their work of phase diagram shows the conversion of CrO<sub>2</sub> to Cr<sub>2</sub>O<sub>3</sub> changes under high oxygen pressure ( $\geq 1$  bar) and high temperature (400-650°C) [26]. From this point of view, the restriction of the low pressure has displayed that Cr<sub>2</sub>O<sub>3</sub> has more stable phase, due to in this work, it has been done under UHV condition. Therefore, under the low pressure to be able to overcome facing the thermodynamically difficulty needs to have special precursor, substrate and appropriate techniques to prepare Cr<sub>2</sub>O<sub>3</sub> thin films.

One of the significant chromium phase is (Cr<sup>4+</sup>) CrO<sub>2</sub>. CrO<sub>2</sub> stability depends on deposition techniques [11], [27], oxygen partial pressure [28], substrate materials [29], temperature [2], [28], even crystal structure orientation [2], [29], [30]. CrO<sub>2</sub> with the proper lattice parameters,  $a = 4.41 \text{ \AA}$  and  $c = 2.91 \text{ \AA}$ , can adapt to rutile crystal structure [31]. While growing of the Cr<sub>2</sub>O<sub>3</sub>, the CrO<sub>2</sub> main peak can be seen. In the following part, where the sample growth and analysis are going to be stated, this feature can be seen from the XPS spectra. It can be seen that either growth CrO<sub>2</sub> or Cr<sub>2</sub>O<sub>3</sub> thin films, the growth parameters are very significant.

To be able to grow the stable Cr<sub>2</sub>O<sub>3</sub> phase, all mentioned parameters are performed for this study. In part three, it will be explained. As mentioned above chromium phases, it could have many phases at the same time, just have one pure phase is quite hard. To obtain the expected phases of the Cr oxide, the growth has been done for several substrate temperatures, different gas pressures were used to obtain desired optimized parameters for Cr oxide growth. In literature, there are many studies have been employed. Such as, under the 1atm oxygen pressure, the stable films obtained between 330°C and 390 °C, and also it depends on substrate materials and orientation [13], [29], [30], [32]. However, for some works the growth has been done even at low substrate temperature which is around 100°C in the vacuum condition [2].

As temperature, vacuum, oxygen and argon gases have effect on stability of Cr<sub>2</sub>O<sub>3</sub> phase, the growth methods also have impact on. There are many growth methods have been used in literature, such as by using MBE [10], [11], [12], Sputter [13] and

PLD [13], [14]. On the other hand, CVD technique can do deposition at the high oxygen pressure and high temperature, more stable CrO<sub>2</sub> thin films were grown [2], [29], [30], [32]. But still it is very difficult to obtain pure CrO<sub>2</sub> phase by CVD techniques. According to Sokolov, the films which were prepared by RF sputtering techniques, analyzed by XRD and XPS techniques, XRD peaks showed that the film consisted of CrO<sub>2</sub> phase, however, for the same sample XPS showed the Cr<sub>2</sub>O<sub>3</sub> peaks [13]. In literature, the most used analysis techniques were XRD and Raman Spectroscopy which have less surface sensitivity than XPS. Therefore, in this work the XPS mainly is employed for analysis of thin films due to high surface sensitivity since decomposition occurs on the top of surface of thin films. Considering that situation, the growth of the CrO<sub>2</sub> cannot be stated as a successful work. One of the other work is that the sample had been taken out to the atmospheric condition, and they reported that the specimen displayed the Cr<sub>2</sub>O<sub>3</sub> phase [12]. Furthermore, the literature study shows that the preparation of CrO<sub>2</sub>, even though CVD techniques show some distinct successful studies, it is not sufficient for technological application. Such that the CrO<sub>2</sub> multiple layer films which prepared for spintronic application result; on the contrary, thermodynamic obstacle, irregular interface, and under the atmospheric condition, the stability could not be obtained, therefore, the expected result was very smaller than the theoretically one [33]-[35].

The importance of the chromium oxide phases has been explained for technological application. In this case, therefore, the metal oxide is the main work of this study. Specifically, this work is devoted to the chromium oxide. The following parts will explain why chromium oxide has been chosen. Another significant event is that the reason of CrO<sub>2</sub> is mentioned here is due to the growth of chromium oxide can be in the form of CrO<sub>2</sub> easily, however, it can transfer to the Cr<sub>2</sub>O<sub>3</sub> phase by post annealing.

Cr<sub>2</sub>O<sub>3</sub> deposition displays very good properties such as high hardness, good wear resistance, low coefficient of friction, chemical inertness, mechanical strength, and also better corrosion and oxidation resistance [36]. Cr<sub>2</sub>O<sub>3</sub>, also, is the hardest material among all the chromium oxides phases. These coatings have been used in many applications, such as corrosion protection, wear resistance, electronics and optics. Since Cr exhibits multiple oxide states (+3, +4, +6), previous studies show that tight control of the oxygen partial pressure and substrate temperature during the evaporation of Cr metal has to be fulfilled in order optimize the growth of stoichiometric Cr<sub>2</sub>O<sub>3</sub>

films. Beside of the ultra-thin film of  $\text{Cr}_2\text{O}_3$ , the bulk  $\text{Cr}_2\text{O}_3$  has close-packed corundum structure ( $a = 4.958 \text{ \AA}$ ,  $c = 13.594 \text{ \AA}$ ) with rhombohedral symmetry [37].

The purpose of this study is controlled growth of  $\text{Cr}_2\text{O}_3$  thin films by RF and Pulsed DC and analyzed with XPS. The  $\text{Cr}_2\text{O}_3$  phase is utilized by RF magnetron sputtering and Pulsed DC magnetron sputtering. Chromium oxides,  $\text{Cr}_x\text{O}_y$ , are popular because of the difference in their applications in variety of fields such as protective coatings for read-write heads in digital magnetic recording units, applications involving corrosion/oxidation resistance, decorative coatings and coatings with specific optical, or electrical properties, and in glass blowing applications. Also, the  $\text{Cr}_2\text{O}_3$  is very good candidates for protection of steel and decorative applications due to its hardness. The oxygen atoms in  $\gamma\text{-Cr}_2\text{O}_3$  crystalline structure (rhombohedral) have a hexagonal close-packed (HCP) arrangement which is known as the corundum structure. The growth of chromium oxide can be done by many variety techniques such as Physical Vapor Deposition (PVD), Ion Implantation, Chemical Vapor Deposition (CVD), and Thermal Spray [38]. The Molecular Beam Epitaxy (MBE) growth technique at a chamber base pressure of  $5 \times 10^{-11}$  mbar was used; the single crystalline  $\text{Cr}_2\text{O}_3$  (111) films were grown on c-plane  $\text{Al}_2\text{O}_3$  substrate by thermal evaporation of Cr metal from a Knudsen cell in an  $\text{O}_2$  background pressure of  $2.2 \times 10^{-6}$  mbar and its substrate temperature was maintained at  $300^\circ\text{C}$  [16].

In this thesis, the aim of the work is to grow the chromium oxide by Pulsed DC and RF Magnetron sputtering and Chromium Oxide centrally be using Photoemission Spectroscopy in surface characterization. In general, there are many other methods to grow  $\text{Cr}_2\text{O}_3$ .  $\text{Cr}_x\text{O}_y$  has many different phases, the other phases have been seen for some studies. Each  $\text{Cr}_x\text{O}_y$  phases have their own properties, and applications.  $\text{Cr}_2\text{O}_3$  study for controllable work and analysis of the  $\text{Cr}_2\text{O}_3$ , and in order to define oxide phase XPS is used. This helps to characterize the electronic properties and chemical stoichiometry of the growth surfaces. The spectrum of the surface will give the ratio of Cr/O. This assures that which chromium oxide phases have been grown and if any other phases exist, their ratio also can be calculated.

The interest in chromium oxide based coatings is motivated by the fact  $\gamma\text{-Cr}_2\text{O}_3$  is insulator, antiferromagnetic, among the hardest oxides, and has many current applications in, e.g., hard coatings, recording media, and spintronic. For wear-resistant coatings,  $\gamma\text{-Cr}_2\text{O}_3$  is also relevant as a template layer for growth of  $\gamma\text{-Cr}_2\text{O}_3$  and  $\gamma\text{-Al}_2\text{O}_3$ . PVD of  $\text{Cr}_2\text{O}_3$  deposition is often employed by RF Sputtering gun, and for

industrial purposes, upscaling is an important challenge. The magnetron sputtering is utilized to be able to transfer this technology to industry.

Many different substrates have been used for  $\text{Cr}_2\text{O}_3$  growth thin films in literature for instance, Ag, Cr, Pt, Si. For this work, Si substrate has been selected. The following step will be done respectively in this study. The Chromium oxide films will be grown in UHV conditions by using Pulsed DC and RF Magnetron Sputtering Depositions. The thickness of films on naturally Oxide Si Substrates vary in range of 20 Å to 200 Å. Si is used due to structure of growth of  $\text{Cr}_x\text{O}_y$  on the Si substrate, the influence of oxygen's partial pressure and substrate biasing on the growth and properties of  $\text{Cr}_x\text{O}_y$  thin films have been reported in the literature. It has been shown that when the number of consumed oxygen atoms equals to the sputtered chromium atoms the deposition process moves from metallic to reactive. However, this one to one ratio causes target poisoning and therefore reduces the deposition rates especially it happens for DC and Pulsed DC. The Pulsed DC is better than DC. It is possible to grow oxidic thin films by Pulsed DC then DC sputter gun. However, with Pulsed DC deposition is not possible for long time. After a while the target gets poisoned and the deposition ratio decreases, finally the deposition rate totally stopped. The restriction of Pulsed DC growth method forces to find out a new method which can do deposition for long term. Generally,  $\text{Cr}_2\text{O}_3$  thin films can be deposited with various technologies including thermal spray [38], sputtering, and ion implantation. Chromium oxide,  $\text{Cr}_2\text{O}_3$ , is a material which has been used for the protective coating of mechanical components due to its outstanding wear resistance. It is generally deposited by RF cathodic sputtering of a chromium oxide target [39]. Even in this study, the RF method is going to be used. It is very good way to deposit the chromium oxide thin films.

## 1.2. Thin Films and Surfaces

In general, the thin films thicknesses are from nanometer to micrometer range. The ultra-thin film growth supplied controlled fabrication of materials. The thin films growth is very significant for technological application due to that it can be acquired and prepared the wanted materials. The thin film has a homogeneous material. Thus makes it appealing for the recent technology. The thin films can be grown on a substrate to deposit on it by many different growth techniques. The percentage of the

material can be controlled. The thin films are employed in the UHV condition, in order to keep the thin films clean by avoiding the contaminants. The deposition of the thin films could be coated on glass, polymers and metals.

The surface of a material displays the characteristic feature of a material, therefore, the surface of the sample is very important. It is because of the surface which can easily contact to the environment. And contact with environment could change the surface structure. Therefore, most of the ultra-thin films growth are being done under UHV condition. The growth chamber and analyzer are connected over load-lock, so the system required to be design as a cluster. So the surface maintains clean ambient by preventing the sample without exposing to the environment.

- Surface Photoemission

Surface photoemission is a method that for probing the material surface chemical composition. This elemental analysis will give the species atoms on surface, concentration of surface atoms and vertical distribution such as on surface or near surface. The surface Photoemission requires a source. In this system the XPS analytic chamber consists of the Twin Anode which consists Mg and Al anodes. The source of the light created by applying the bias to the filament then filament emits the electron, and this electron hits the either Mg or Al anodes depends which is going to be operated. The X-ray goes through the aluminum window to decrease bremsstrahlung irradiation. The source of light from the either from Mg  $K\alpha$  (1253.4 eV) or Al  $K\alpha$  (1486.6 eV) will hit the specimen and ejected core electron which consists idea of the element. Another method can be used to analyze the specimen by X-ray is synchrotron. In synchrotron, kinetic energy is from 0.1 to 5 keV. The light penetrates the sample depends on its energy. Another more important thing is the inelastic mean free path (IMFP) which is the average distance between inelastic collisions. The IMFP depends on kinetic energy and it is higher for low kinetic energy. Besides of this, while these methods are surface sensitive, below the surface where X-ray could not penetrate the sample, the sample can be sputtered, then the composition of the sample below can be defined.

The photoemission spectrum depends on core level electron binding energy. S orbitals do not have spin-orbit splitted due to its  $l = 0$ . And it is singlet in XPS. However, for  $l > 0$ , p, d, f..., orbitals are spin-orbit splitted, therefore, they are doublet in XPS. Besides of the XPS, the Auger peaks always accompany the XPS. The Auger



electron occurs when the core electron ejected by the x-ray the above level electron relaxation, the amount of that energy release. This energy will eject an electron and this electron's kinetic energy is independent from the source energy. Therefore, to probe a real peak can be controlled by this feature using two different sources. If it is a real peak it would stay the same otherwise it would either shift or vanish. The equation (1.1) gives the binding energy ( $E_B$ ).

$$E_B = hv - E_k - \Phi \quad (1.1)$$

The XPS data analysis is read by  $E_B$  because, the elemental analysis of the sample, the characteristic of the atom feature depends on the binding energy. Binding energy gives the element and the binding energy shift defines the chemical component. Where  $hv$  is the photon energy from the source,  $E_k$  is the kinetic energy of the ejected electron from the core shell of surface specimen.  $\Phi$  is the spectrometer work function. While one of the core state remains abundant, that should be filled by above electron. One of the electron from the above level fills that hole, the amount of relaxation energy emits that energy could eject an electron. That electron is called Auger electron. Dependent on Auger electron energy spectrum analysis is known Auger electron energy spectrum (AES). And it does not dependent on source energy.

$$\lambda_a = \frac{538a}{E^2} - 0.41a(aE)^{0.5} \quad (1.2)$$

The analysis of the sample with XPS and AES spectra are taken from the surface. The photon penetration in sample is dependent on attenuation length ( $\lambda_a$ ) of electron which is dependent on the inelastic mean free path (IMFP). The relation of  $\lambda_a$  in material is seen in equation (1.2). In equation (1.2), where  $E$  is the energy of the electron in eV,  $(a)^3$  is the volume of the atom in  $\text{nm}^3$  and  $\lambda_a$  is in nm [40]. By being surface analysis with XPS that one of the merit of the XPS is that it is not surface destructive [41]. Therefore, it is used widely to characterization of ultra-thin films.

### 1.3. Outlines

In this work, the information which is mentioned in the above is all about the importance of the ultra-thin films and their growth and analysis system. Due to its wide range technological application and merit of it. The chromium oxide growth is performed by magnetron sputtering and analyzed by XPS. There are couple substrates used for  $\text{Cr}_2\text{O}_3$  growth thin films. Natural oxide silicon crystal (100) is used as substrate in this study. This silicon piece was cleaned with ethanol before mounted in the load lock. The sample, initially growth with Pulsed DC magnetron sputtering. The sputtering gas is Argon and for growth of oxide thin films, the oxygen is sent to the chamber. The thin films of the  $\text{Cr}_2\text{O}_3$ , is affected from the substrate temperature, gas partial pressure and post annealing. These all parameters were employed to find the optimized parameters for growth. Because for the thin film growth the argon oxygen pressure have influence on the film structure [42]. After determine the Pulse DC magnetron sputtering parameters, then the RF magnetron sputtering has been performed. The parameters have been sought here also. Each film growth thickness was controlled by QCM. Moreover, the thin films spectrum has been taken after each growth by XPS. The XPS has been chosen due to the surface sensitivity. It gives the information of chemical composition of surface. Which elements are there and what are their ratio can be calculated. The following part will explain whole study which is briefly mentioned in the above.

## **2. EXPERIMENTAL TECHNIQUES**

### **2.1. Thin Films Preparations**

In this part; the thin films specimen's growth and analyzer techniques will be discussed. Due to the mandatory of the preparation of ultra-thin films is required a clean ambient, thereby these samples are prepared under UHV (Ultra High Vacuum) condition with magnetron sputtering. The UHV condition is necessary requirement for the growth chamber and the analytical chamber which both are combined over a load-lock chamber to build a cluster chamber; so that the film growth processes and characterizations are done in-situ for this work. The growth and analysis system will be stated respectively in following sections.

#### **2.1.1. UHV Cluster Chambers**

It is required that the chamber should be kept in the UHV condition in order to avoid contamination during growth and analyzing of the samples. The UHV condition was obtained by Advanced Ion Pump and Turbo Molecular Pumps (Pfeiffer Brand) supported via foreline by Mechanical Pump. The Turbo Molecular pump is supported by a mechanical pump to obtain high vacuum where is used to obtain high vacuum in the growth chamber. The Cluster system packed by the growth and analyzer chambers with full equipped is shown in Figure 2.1 which has been bought from the BESTEC Company. One of the significant pumps is Ion pump that is using to obtain and maintain UHV condition for the XPS analytic chamber which able to reach  $10^{-10}$  mbar. The ion pump basically works by ionizes the gas within the vessel that it attaches to and applies a strong electrical potential, generally it is around 5 kV, which allows the ions to accelerate into and be captured by a solid electrode and its residue. Another pump is used in XPS analytical chamber is titanium sublimation pump (TSP) that can be used as a component of ultra-high vacuum systems. The operation of TSP is based on a titanium filament through which a high current is passed periodically. This current causes the filament to reach the sublimation of titanium, and hence the surrounding chamber walls become coated with a thin film of clean titanium. Since clean titanium is very reactive, components of the residual gas in the chamber which collide with the

chamber wall are likely to react and to form a stable, solid product. So the gas pressure in the chamber is diminished.

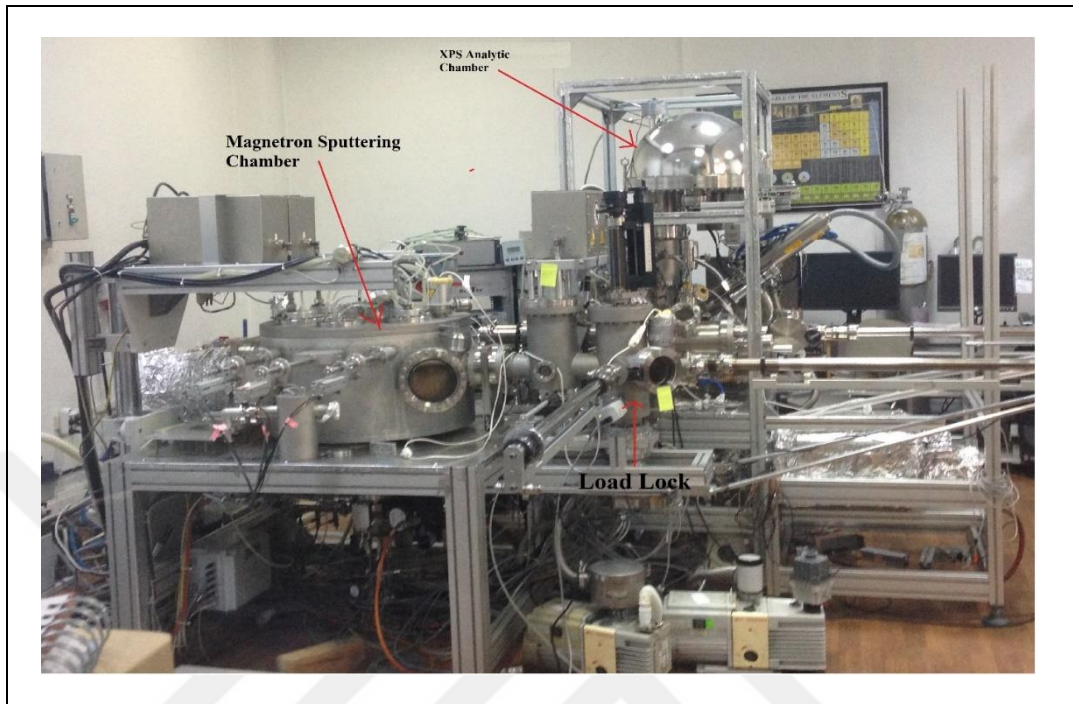


Figure 2.1: Magnetron sputtering and XPS analytic chamber.

In a UHV chamber the turbomolecular pump (TMP) is very crucial to obtain and maintain ultra-high vacuum. For an efficient TMP, the foreline needs to be in low pressure therefore the TMP pump generally supports by a mechanical pump as it shown in Figure 2.2. So, the chamber vacuum base could be maintained around  $10^{-9}$  mbar.

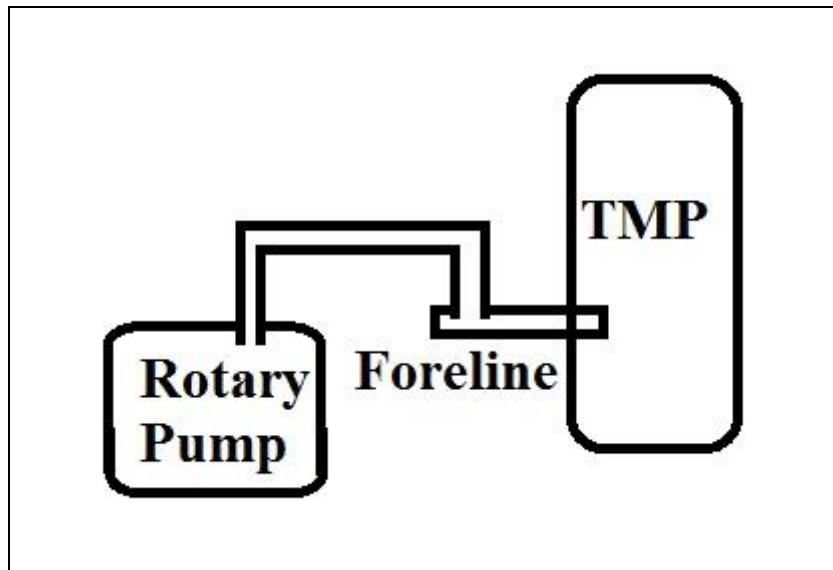


Figure 2.2: The schematic view of Turbomolecular (TMP) and Rotary Pumps are combined by Foreline.

Moreover, Turbomolecular pumps sweep out a larger area than mechanical pumps. and TMPs do so frequently, thus making them capable of much higher pumping speeds. They do this at the expense of the seal between the vacuum and their exhaust. Since there is no seal, a small pressure at the exhaust can easily cause backstreaming through the pump. Therefore, the exhaust should be in low pressure. In high vacuum, however, pressure gradients have little effect on fluid flows, and molecular pumps can attain their full potential. Turbomolecular pumps will stall and fail to pump if exhausted directly to atmospheric pressure, so they must be exhausted to a lower grade vacuum created by a mechanical pump. Therefore, as it is displayed in Figure 2.2. the turbomolecular pumps backs up by mechanical pump. The mechanical pump is connected to the venting connection of turbomolecular pump to provide a low pressure or a vacuum to support turbomechanical pump efficiently. Furthermore, besides the turbomolecular pump, Cryopump (Leybold Brand) can be used instead of turbomolecular pump to obtain ultra-high vacuum. This pump also needs mechanical pump for back up. After regeneration the residual gas pump out by helping of the mechanical pump.

In conclusion, the ultra-thin film studies require UHV, and also in situ growth and analysis is very crucial because of avoiding of the contamination. Thus this system is built as a cluster system. These two different systems have been connected by a load lock as it can be seen in Figure 2.1. Initially, the samples mounted to the load lock.

The load lock can have ten samples at one time. Then the load lock is vacuumed. When the load lock vacuum reaches the UHV, the sample can transfer to the growth chamber by transfer arm. After the growth completed, by transfer arm the sample transferred to the load lock. And then the sample again by the transfer arm which can sample transfer to the XPS analytical chamber for elemental analysis. By following these steps, the sample without exposing to the air. The sample is prepared in situ. The base pressure of the growth and analytical chamber are maintained by the connected pumps which are mentioned before.

### **2.1.2. Substrate Preparation Before Growth Process**

Before growth process has been started, there are some processes that need to be followed to make a sample with well defined-surface. The well-defined surface leads to grow the controllable thin films on substrate. Undefined surface would bring some problems which would not be determine due to the not well-define surface, because the problems can be either from the surface or external conditions such as gas pressures, temperature, and applied bias. To be able to define a well surface, the following process has been employed to the natural oxidized single silicon crystal (100). Another important part is that a clean and well defined specimen needs a clean environment both the growth and analytical chamber, so the chamber needs to be in UHV condition which is explained above in detail. That is provided to establish clean conditions for the preparation of a well-defined solid surface or the performance of in situ studies on a freshly prepared interface.

In this study, naturally oxidized silicon (100) single crystals are used as the substrate. The piece of polished Si single crystal is cleaned and mounted on holder. The Si crystal substrates are cleaned in ultrasonic bath. Then the specimen is flushed with ethanol. The sample is ready to mount on the sample holder. Then it can be transferred to the load lock. The sample is cleaned to avoid any residue from ambient. This cleaning process has been done outside of the system.

When the sample mounted to the load lock, then system is closed then it is pumped. When the load lock reaches the UHV, the sample can be transfer to the chamber for growth. Another cleaning process applied here to remove any adsorbent contamination on the substrate, so the sample is heated up to 600°C by a Pyrolytic

Boron Nitride (PBN) heater. This heater is mounted on the manipulator. This heater can do the thermal radiation in UHV condition, so the specimen can heat up the sample to the desired temperature. Another process is etched or sputtered the substrate to clean the surface. The etching is placed between load lock and growth chamber. The sputter gun is placed in analytic chamber. One of the important part is etching process which is very crucial to clean the substrate. The etching is mounted between the growth chamber and load lock. In addition, there is a sputtering system is mounted in Analytical chamber to clean the surface.

The surface of the substrate is defined by XPS or LEED. XPS provides the elemental analysis of the surface to assure that there is any contamination on the surface. XPS has about 5 nm sensitivity. LEED is working differently compare to the XPS. LEED illustrates the crystal structure. It has a very surface sensitivity. Its sensitivity is around 1-2 layer. There are many other advantage of the magnetron sputtering will be discussed in the following.

Furthermore, the sample growth is obtained in the UHV chamber, before starting the deposition, the pressure of the chamber was less than  $5 \times 10^{-9}$  mbar. Basically, the magnetron sputtering growth is working by sending argon gas in to the chamber, because sputtering gas is often preferred as an inert. However, the reactive gas also can be used. There is disadvantage of the reactive gases as being used for sputter gas, because they can contaminate the sample surface. Therefore, in this work argon gas was used. Gases which are used in this system, are not directly feed through the system. Before feeding through the system gases filtered then feeding to the chamber. The argon is used to sputter the target. It works by applying bias to the target, the ionized  $\text{Ar}^+$  hits the Cr target, then ejected Cr deposits to the Si substrate by field force. The oxygen is fed to the system during the growth. Due to the main purpose of this work is to growth  $\text{Cr}_2\text{O}_3$ , therefore, while growing Cr on the Si substrate, the oxygen also is fed into the chamber for obtain  $\text{Cr}_2\text{O}_3$  phase. The merit of the sputter is let to grow the controllable thickness of thin films.

## **2.2. Magnetron Sputtering Thin Film Deposition**

The magnetron sputtering system has capabilities to grow the film thickness in range of the angstrom to micrometers thickness growth to fabricate multilayer

deposition. The magnetron sputtering is a mechanism by which atoms are removed from the surface of a material as a result of collision with high-energy particles. The magnetron sputtering is a physical vapor deposition (PVD) technique wherein atoms or molecules are ejected from a target material by high-energy particle bombardment so that the ejected atoms or molecules can accumulate on a substrate as a thin film. It is a very widely used method for deposition method that can have variety target materials such as Al, Au, Cu, Cr, Ti and Pt.

The reactive magnetron sputtering system is mainly working by magnetrons make use of the fact that a magnetic field configured parallel to the target surface can constrain secondary electron motion to the vicinity of the target. The magnets are arranged in such a way that one pole is positioned at the central axis of the target and the second pole is formed by a ring of magnets around the outer edge of the target. This holds the electrons in this way significantly rises the probability of an ionizing electron-atom collision occurring. The increased ionization efficiency of a magnetron results in a dense plasma in the target region. This, thereby, leads to increased ion bombardment of the target, giving higher sputtering rates and, therefore, higher deposition rates at the substrate. In addition, the increased ionization efficiency achieved in the magnetron mode allows the discharge to be maintained at lower operating pressures ( $\sim 10^{-3}$  mbar) and lower operating voltages than is possible in the basic sputtering mode [43].

In magnetron sputtering the applied power can be manipulated. The applied power has influences on particle size and deposition ratio. While with high power value the big particles are ejected, the low power is ejected small particle size that has a very uniform homogenous thin films. Thereby, while growth any sample with magnetron sputtering, attention should be paid for the applied power. It causes the thin films uniformity and quality.

Moreover, the sputter system is a physical vapor deposition system that sputtering process consists a target (or cathode) plate is bombarded by energetic ions generated in a glow discharge plasma, situated in front of the target. The bombardment process causes the removal or sputtering of target atoms, which may then accumulate on a substrate as a thin film. Secondary electrons are also emitted from the target surface as a result of the ion bombardment, and these electrons play an important role in maintaining the plasma [43].



As it is displayed in Figure 2.1. The magnetron sputtering chamber consists of the six target guns. Two of them are RF, three of them are DC, and the other one is Pulsed DC. The target guns are parallel to the sample holder. Even it is also parallel to the sample during growth. The sample is prevented from the contamination of initial target sputtering by shutter. Before any growth has been started, initially the target needs to be cleaned by feeding the chamber by argon gases to sputter any contamination on surface.

As it is mentioned above the growth chamber has three different sputter guns to do deposition. RF is one of the method that generally is using for insulators and magnetic materials. However, with the DC is not possible to grow the insulating material due the charge formation on the target surface. This causes the target poisoning. When the target is poisoned, the growth slowly decreases and finally stop. DC sputter gun is used for conductive materials. And also, it is very fast compare to the RF. One of the other sputter gun method is Pulsed DC sputter gun. Which is alternative to the RF and DC sputter guns. It can be used instead of both methods. And it has a frequency between ranges of 10 to 100 kHz.

In addition, the gases which are used in this system are very clean. Even they are very clean, still need to be filtered. The gases which is going to be used, before feeding through the chamber, the gases filtered which is heated about 300 °C. The gases purity clarified by residual gas analyzer (RGA) to assure that the gas does not consist any contamination. The RGA is a mass spectrometer which is using for controlling the UHV chamber system to monitor the contamination or any leakage.

As it is already aforementioned the magnetron sputtering. The magnetron sputtering is very beneficial method to grow the ultra-thin films. It has many advantages that is going to be discussed. Basically, the magnetron sputtering consists of magnets. Magnets are used to increase the percentage of electrons that take part in ionization phenomena which is very crucial for growth. They increase probability of electrons striking argon, and increase electron path length, so the ionization efficiency is increased significantly.

There are many reasons that the magnetron sputtering is picked. Some of the reasons are;

- Low plasma impedance and thus high discharge currents from 1 A to 100 A.
- Coating rates in the range from 0.1 Å/s to 10 nm/s. And it can be control.

- Low or high thermal load to the substrate.
- Deposition uniformity.
- Dense and well adherent coatings.
- A wide range of target materials.
- Sample holder can be heat up by PBN.
- Sample holder can be cool down by cooling system [44].

Due to the merit of magnetron sputtering, the magnetron sputtering is used for the ultra-thin films growth. The magnetron sputtering can be easily used in industrial. Because it is possible to use a large target and substrate to grow. Therefore, it is very important to be able to make any new materials and able to use in industrial application. Moreover, it is used in industrial work due to the reasons mentioned below and also magnetron sputtering can be used for large areas. Furthermore, because of its advantages magnetron sputtering is a coating technique widely used for large areas such as deposition of optical, metallic and hard coatings application [45].

Besides of the advantage of the magnetron sputtering, there are some main parameters that need to be paid attention:

- Argon pressure
- Sputter voltage
- Substrate temperature
- Substrate to target distance
- Deposition time

These parameters are very significant while operating the system to pay attention to grow a perfect thin films. Any of the above parameter changes can affect the thin films. Their effects can be seen in our thin film of Cr oxide. Helium is also can be used instead of argon gas for sputtering. It is not used widely due to its cost. It is very expensive. Therefore, researchers commonly use argon as a sputtering gas. Alternatively, for reactive magnetron sputtering other gases like oxygen or nitrogen are fed in to the sputter chamber additionally to the argon, to produce oxidic or nitridic films. During growth of Cr on Si substrate the oxygen is fed in to the chamber.

Furthermore, during growth the oxide and nitride thin films, argon, oxygen and nitrogen partial pressure is also significant to obtain a perfect thin films.

Reactive magnetron sputtering chamber which is used in this work is fabricated by BESTEC which has 2 RF, 3 DC and 1 Pulsed DC that has 3 inches diameter Magnetron Sputter Guns and work in UHV condition with base pressure  $< 5 \times 10^{-9}$  mbar. The deposition is made in this chamber which can deposit oxide films by Magnetron Sputtering. Due to the DC sputter gun poisoning issue the best growth acquisition performed parameters has been probed by RF and Pulsed DC in this work. Even the Pulsed DC can be poisoned after long time exposed to the oxygen. The  $\text{Cr}_2\text{O}_3$  thin films have been employed by both methods.  $\text{Cr}_2\text{O}_3$  thin films are obtained by the pure chrome target which positioned in the RF source place and Pulsed DC source place, the growth is happened by giving the system argon and oxygen gases. The growth samples thickness is monitored in situ by Quartz Crystal Microbalance (QCM) which is mounted on the movable sample holder. In addition, to prepare and after preparation the specimen annealed by PBN heater which is also mounted on movable sample holder.

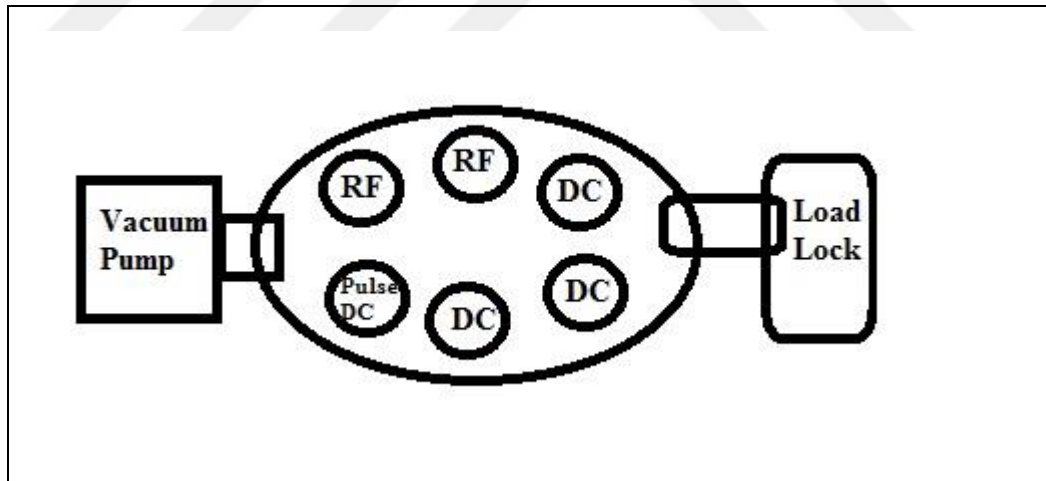


Figure 2.3: The schematic view of Magnetron Sputtering Chamber: RF, DC, and Pulsed DC sources. Vacuum Pump and Load Lock.

### 2.2.1. DC Magnetron Sputtering Process

By DC-Magnetron Sputtering, practically as it is mentioned before, a negative potential  $V$  up to about 100 Volts can applied to the target. As a result, the argon-ions are accelerated towards the target and set material free by hitting the target material,

on the other hand they produce secondary electrons. These electrons cause a further ionization of the gas. DC Magnetron Sputtering is faster method among magnetron sputtering methods. However, for oxidized samples, it is hard to grow thin films. Because, DC target either poisoned or arcs can occur. Therefore, growth with DC sputter gun would not allow to grow the thin films. Because, if the target is poisoned, the growth would stop.

### **2.2.2. Pulsed DC Magnetron Sputtering**

One of the other method of magnetron sputtering is Pulsed DC power. It is widely used for reactive magnetron sputtering, particularly for dielectric materials. While it was not possible do dielectric materials growth with DC sputter gun. This issue is solved by Pulsed DC. This was carried out by periodically discharging the voltage on dielectric films reactively deposited on the target, actually preventing the occurrence of arcs. Due to that property it can be alternative to the DC restriction. The concept of voltage reversal to prevent target arcs during reactive sputtering. An important aspect of this development was the use of voltage reversal as an effective way to handle the few arcs that did occur. It is fast compare to the RF sputter gun. Even it can be used for chromium oxide thin films, the Cr target can poison for a long time exposing to the oxygen.

### **2.2.3. RF Magnetron Sputtering**

Another method of the Magnetron Sputtering is RF sputtering gun. The problems which are faced with DC and to be solved with Pulsed DC have been tried to overcome with RF sputter gun. Still most of the problems could not overcome by DC and Pulsed DC sputter guns, such as arcing, oxidation and charge accumulation on the surface. Therefore, RF magnetron sputtering is suggested for deposition to handle this kind of problems which are already mentioned. The bombardment of a non-conductivity target with positive ions would lead to charging of the surface and subsequently to shielding of the electrical field. The ion current would die off. Therefore, DC sputtering is restricted to conducting materials like metals or doped semiconductors. In RF sputtering gun an AC-voltage is applied to the target. In one phase charge neutrality is

achieved. Hereby also sputtering of a non-conducting materials is possible. Both conducting and non-conducting materials can be sputtered. Therefore, the dielectric films can be growth. And also higher sputter rate at lower pressure can be obtained by RF Magnetron Sputtering.

All three methods have been discussed above that need a UHV system, thereby, before deposition the sputtering chamber was evacuated with a turbo-molecular pump down to a base vacuum pressure of less than  $5 \times 10^{-9}$  mbar and also it is possible to use cryopump instead of turbo-molecular pump to obtain that vacuum level. Prior to each deposition run the target was cleaned for 10 min by pre-sputtering in argon atmosphere. During the cleaning process of the target, the sample covered by the shutter which was monitored from the computer. During the growth the shutter draws off that let the substrate exposes to the target ejected materials. Therefore, the target materials are accumulated on the substrate uniformly.

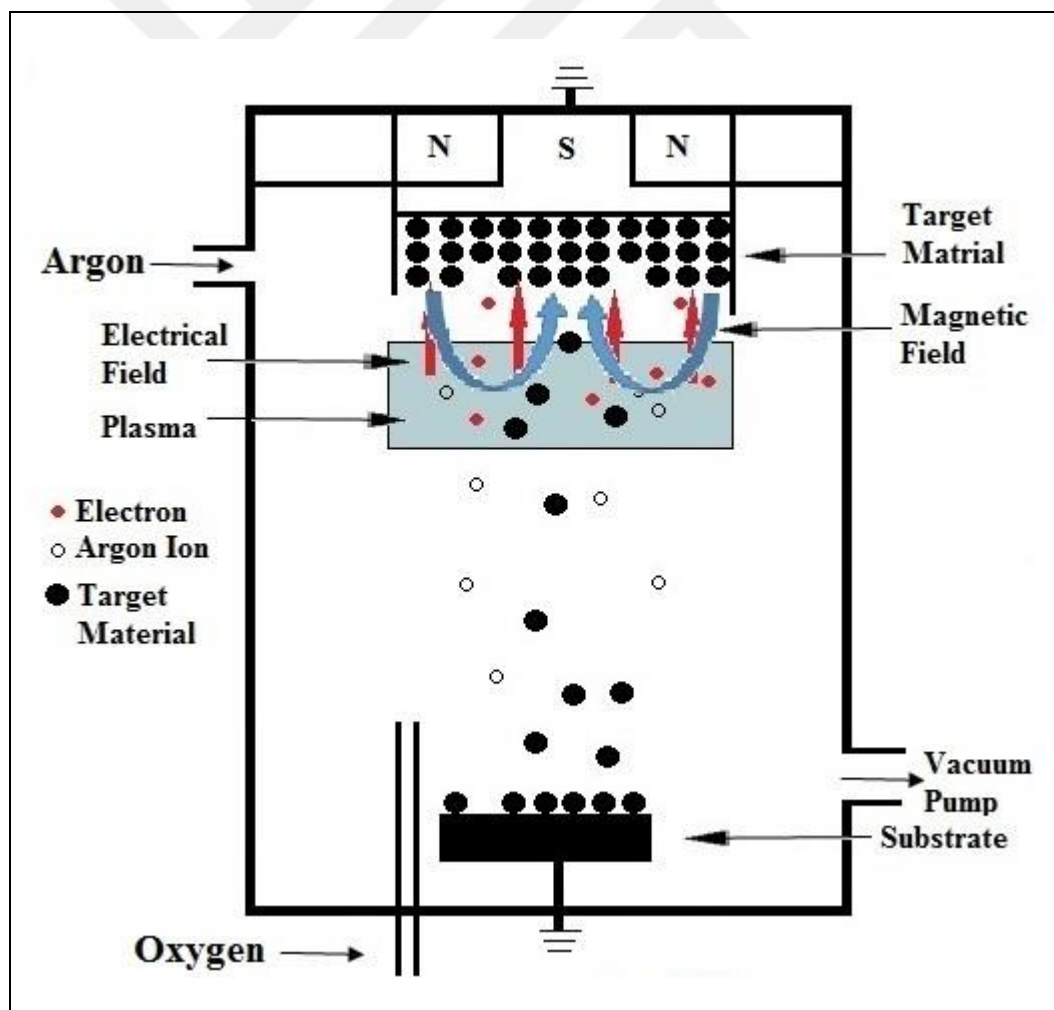


Figure 2.4: Magnetron Sputtering Plasma and Coating Process.

The magnetron sputtering as it is shown in the Figure 2.4, displays the common events of plasma and coating process. The targets are placed on upper side and substrate holder is in the bottom side. The sample holder can move up and down and it is also rotate under the targets. The sample can be heated by a PBN and also there is a cooling system that cools the sample holder. The QCM is mounted to movable holder that it provides information about the thickness of the thin film. After sample transferred to the chamber, before starting to grow to get a homogenous thin films, the target needs to be cleaned. Therefore, initially the sample is obscured by shutter. The bias is applied to the target then the sputtering has been started. Any contamination or oxidation on the target would be removed. After this process the sample growth has been started. The sample growth has been controlled by QCM in-situ. The QCM is selected due to its well-established technique for detecting physical feature of thin layers deposited on the crystal surface on the angstrom range. The QCM is very sensitive to detect the thickness. It measures the change of the frequency of a quartz crystal resonator which gives information about the mass variation on surface. To obtain a very high sensitive QCM, it is calibrated with XPS.

### **2.3. X-Ray Photoelectron Spectroscopy (XPS)**

The growth of the samples is done by reactive magnetron sputtering. The growth of the thin films is very significant and delicate. While growing the ultra-thin films by magnetron sputtering, the thickness is controlled by QCM. However, the chemical composition is needed to be define, therefore, the specimens transferred to the XPS analytical chamber. The analysis of the sample assures that the expectation of the growth will be confirmed to rich. In this work, XPS is used to analyze the sample to examine the Cr oxide phases. Basically, XPS, providing the information about the occupied electronic levels below the Fermi level, is a modern technique with high surface sensitivity ranging up to 10nm. Briefly, XPS based on photoelectron effect. Spectroscopic method, the sample which exposed to light, then the electron called photoelectrons eject from the core level electrons. They are detected by a charge analyzer within the function of their kinetic energies.

XPS is a state of art instrument that is used almost all elements to analyze except hydrogen and helium. Furthermore, the XPS is also called ESCA (electron spectroscopy for chemical analysis). XPS mainly interested in core electron. In XPS, there are some feature that is very significant parameter that to analyze the spectroscopy. Each element has its own characteristic binding energy associated with each core atomic orbital. Therefore, each element gives rise to a characteristic set of peaks in the photoelectron spectrum at kinetic energies determined by the photon energy and the respective binding energy. The presence of peaks at particular energies, therefore, indicates the presence of a specific element in the sample under study, furthermore, the intensity of the peaks is related to the concentration of the element within the sampled region. Thus, the technique provides a quantitative analysis of the surface composition. This gives the ratio of element and their chemical bound relation.

### **2.3.1. Instrumentation for XPS**

As explained the spectrum of XPS has very significant role for define the elements. Besides of that, the instrumentation is also very important, therefore, in this part the instrumentation will be discussed. The Figure 2.5 is a block diagram of a typical XPS spectrometer and its brand is SPECS. The basic components of the system are an X-ray source, a sample, an electron monochromator, a detector, a scan, and readout system. Since it is necessary to ensure that the mean free path of the photoelectron is large enough to allow it to traverse the distance from the sample to the detector without suffering energy loss, XPS requires a vacuum technique with a maximum operating pressure of approximately  $5 \times 10^{-8}$  mbar for long operation life time and suppressing background noises on spectrum. Therefore, the base pressure of the XPS analytic chamber is around  $10^{-10}$  mbar.

The X-ray tube consists of a heated cathode at high negative potential and a water-cooled anode maintained at ground potential. Since the major contribution to the FWHM of a photoelectron line is the inherent width of the X-ray line, such as Mg  $K_{\alpha}$  and Al  $K_{\alpha}$  with a half-width of approximately 1 eV are usually employed for photoelectron excitation. With x-rays, the FWHM of the photoelectron line is minimized. It is possible to further reduce the width of the exciting X-ray and thus the

photoelectron line by using a crystal disperser to provide perfectly monochromatic X-radiation.

Another important part is physical technique of XPS which is going to be define in this section. The vacuum technique is very crucial for XPS analytic chamber. The low vapor pressure solids are most easily run in the vacuum. On the other hand, the easily evaporated materials can release gases in to the chamber that would pollute the chamber. A solid sample needs only be placed on a probe that is appropriately positioned relative to the X-ray beam and the spectrometer slit. Although the exciting X-rays can penetrate deeply into the solid sample, not all of the ejected electrons will escape for ensuing analysis. Those electrons ejected at considerable depths will lose all kinetic energy through internal collisions. For instance, the escape depth of the Au (4f) electrons has been determined to be on the order of 10-20 Å. So XPS is a surface technique. This places no restriction on the surface chemist. However, if bulk properties are to be measured, the surface must have a valid representation of the bulk.

As a consequence of the XPS samples only the first few angstroms of a solid sample, contamination and oxidation of the surface must be minimized. Otherwise, the thin film of the sample would not be examined correctly. Oxidation can be a particularly serious problem if one is studying metals. Contamination by hydrocarbons during sample preparation or by deposition of residual vapors inside the sample chamber is routinely observed on most samples. Ion sputtering techniques are a convenient method for cleaning metallic samples. However, sputtering of powdered samples must be performed with care [46].



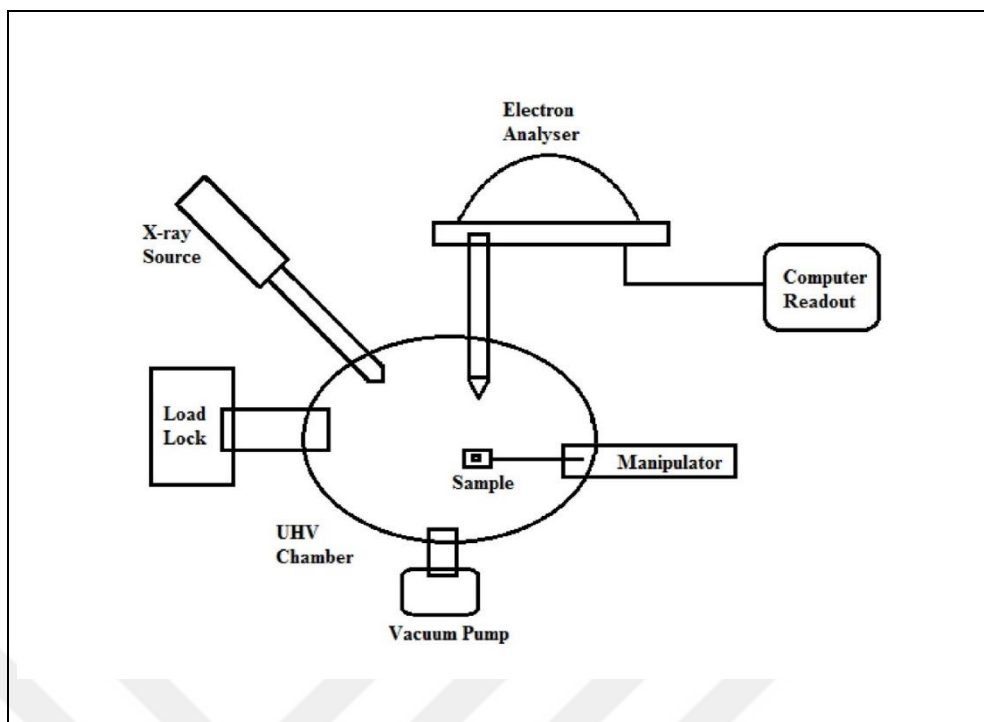


Figure 2.5: X-ray Photoelectron Spectrometer Analytic Chamber.

As it can be seen Figure 2.5 displays the XPS system. The load lock holds the samples which prepared in the magnetron sputtering, and then they are transferred to the XPS chamber for analysis without exposing to the environment. The manipulator, which has five axes, helps to position the sample in front of the XPS.

### 2.3.2. Photoemission Mechanism

Another important part of the XPS system is data readout. The chromium electron configuration is  $1s^2 2s^2 2p^6 3s^2 3p^6 4s^1 3d^5$ . The initial point of analysis chromium oxide is done by analysis of Cr2p spectra which is the separation of  $2p_{3/2}$  and  $2p_{1/2}$  spin-orbit split components. Which is very significant point that to understand and characterize the elements. In most cases, this separation is large enough to consider only the more intense  $2p_{3/2}$  signal and its associated structure. This feature of the spin-orbit split components can be seen in Cr2p spectra. Moreover, a primary objective of the interpretation of Cr2p XPS spectra is usually to determine the relative percentages present in the 0, II, III, IV and VI oxidation states in order to follow oxidation processes. These different oxidations of the Cr phases have their own 2p binding energy. That feature can be seen in part 3.

Analysis of the X-ray photoelectron 2p spectra of the first row transition metals is challenging due to peak asymmetries, complex multiplet splitting, shake-up and plasmon loss structure, and uncertain, overlapping binding energy positions. Looking at details of the XPS work process, Figure 2.6 will clarify the physical events of the XPS.

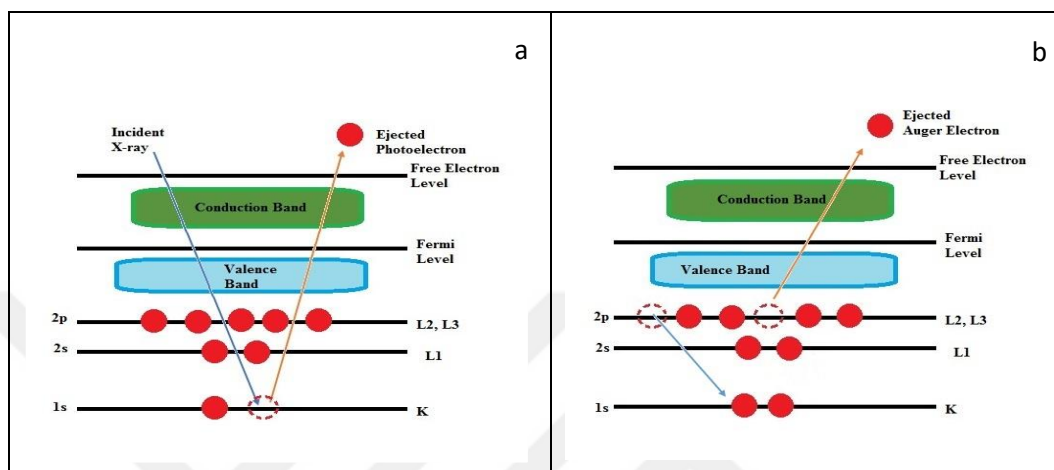


Figure 2.6: a) Photoelectron effect and b) Auger process.

X-ray photoelectron spectroscopy as it explained above, its physical process is explained in Figure 2.6. In the XPS, incident X-ray which is created in the source by either Al  $K\alpha$  or Mg  $K\alpha$ , the created x-ray emitted to the specimen and eject the specimen's core electron as it is displayed in Figure 2.6. The ejected core electron is detected by analyzer. The ejected photoelectron causes an unoccupied orbital, that orbital will be occupied with high orbital electron, then electron will release an energy. If that energy can eject an electron, this is called Auger electron. That electron can also be seen in the spectrum. This feature is also gives the information about the elements. And also Auger electron does not depend on the kinetic energy. Using different source to characterize sample spectrum's Auger peaks won't change if it is real.

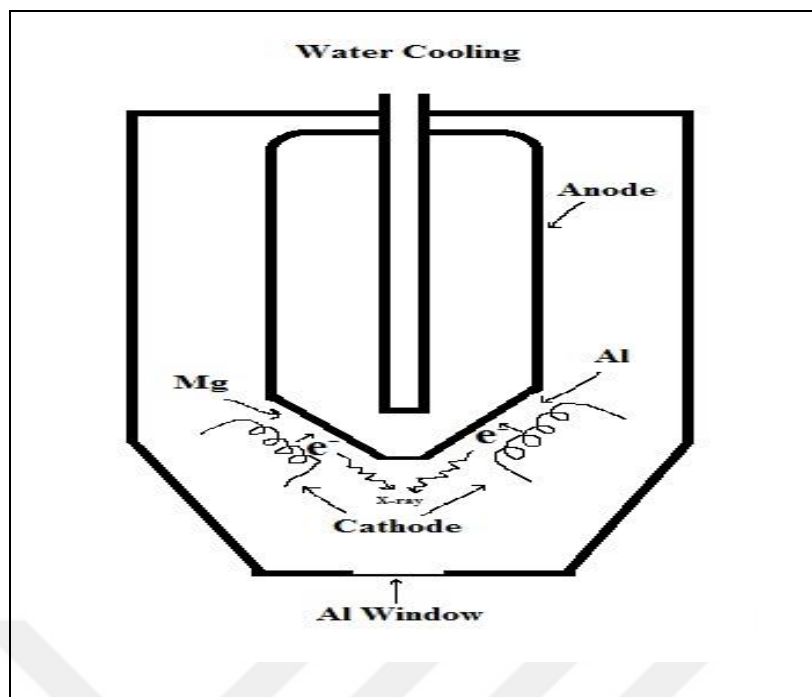


Figure 2.7: X-ray source, twin anode (Al, Mg).

The most commonly employed x-ray sources are those giving rise to: Mg K $\alpha$  radiation:  $h\nu = 1253.6$  eV and Al K $\alpha$  radiation:  $h\nu = 1486.6$  eV. Technically, in the source part the tungsten emits electron by applying the voltage as it is seen in Figure 2.7. These emitted electrons hit the Mg or Al anode, they eject electron from the anode materials. The ejected electrons leave unoccupied orbital. This unoccupied orbital level, is filled by the high orbital level electron. While this electron drops to lower level emits the X-ray. That X-ray which is sent to the sample. By using the Mg or Al anode, the emitted photoelectrons will therefore have kinetic energies in the range of 0 – 1250 eV for Mg K $\alpha$  and 0 – 1480 eV for Al K $\alpha$ . Since such electrons have very short IMFPs in solids, the technique is necessarily surface sensitive.

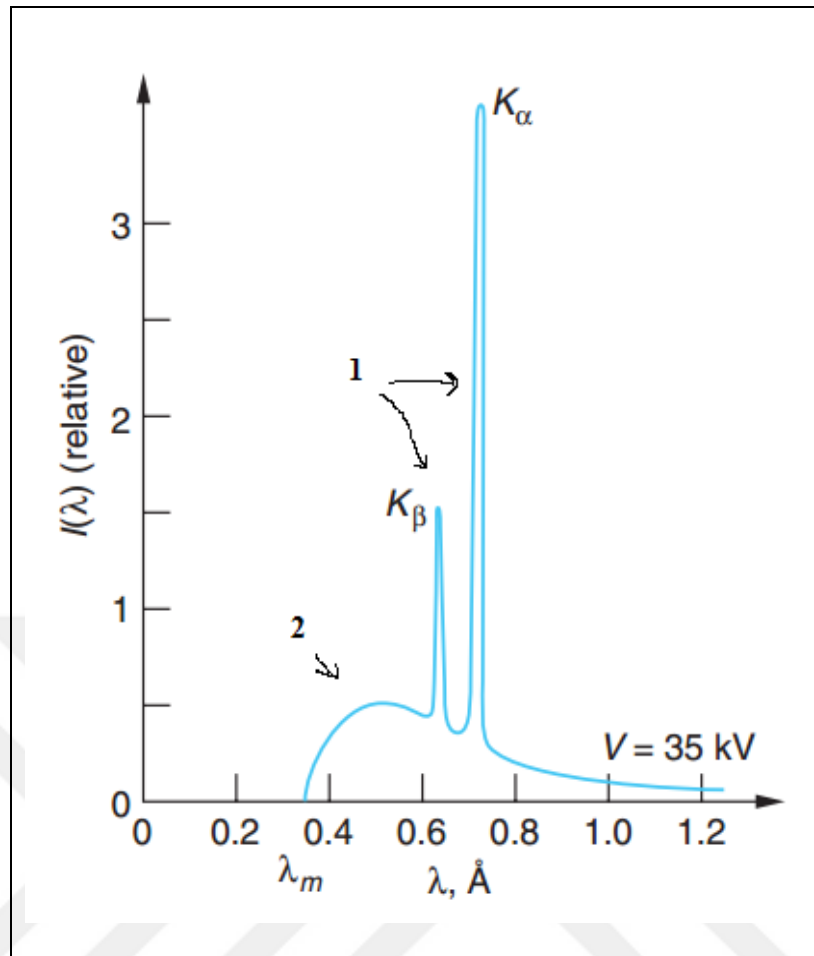


Figure 2.8: Characteristic & Bremsstrahlung radiation. 1) The spectrum consists of a series of sharp lines, called the characteristic spectrum, superimposed on 2) the continuous bremsstrahlung spectrum.

As it is mentioned, the X-ray source has some property that as it is illustrated in Figure 2.8 [47]. There is a characteristic feature that it is due to its electron configuration of Al and Mg are  $K_{\alpha}$  and  $K_{\beta}$ . The Bremsstrahlung radiation is continuous phenomenon. To reduce Bremsstrahlung radiation, the Aluminum window is used.

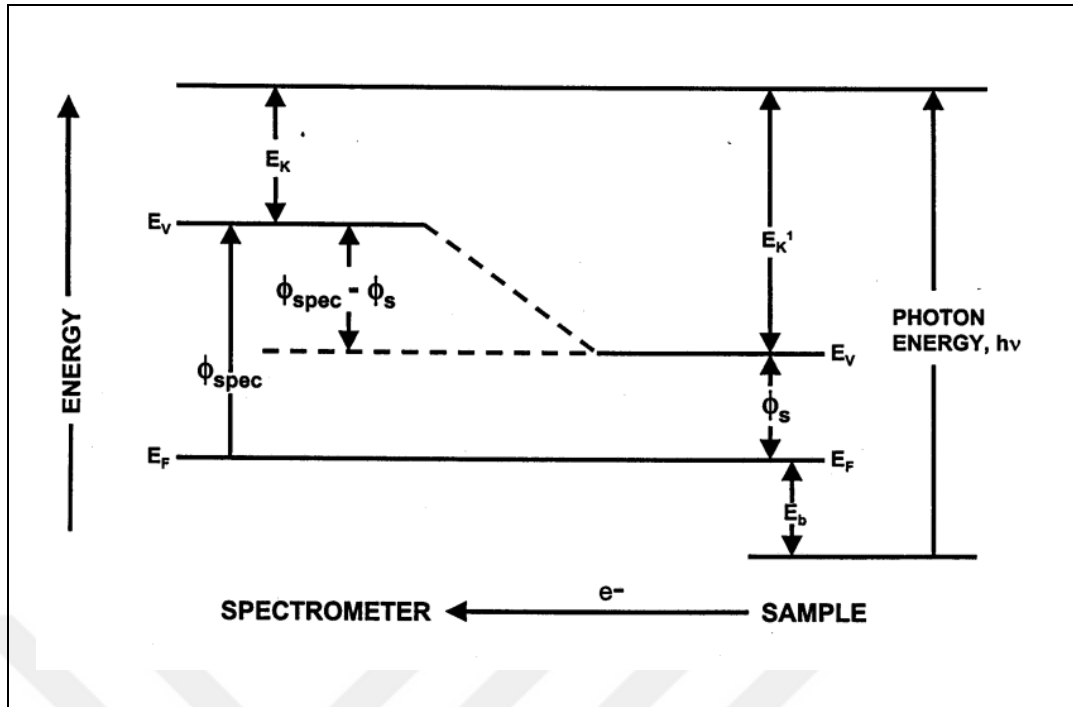


Figure 2.9: Energy level schematic for XPS binding energy measurements.

Another important part is photoemission which helps to characterize the materials. Photoemission process happens as in Figure 2.9 [48]. The emitted X-ray ejects either valence band's electron or core electron. And the ejected electron moves through to the detector as shown above photoelectron energy diagram. Conductor and spectrometer are electrically contact to each other. Therefore, both spectrometer and photoelectron energy needs common reference. That reference is called fermi level,  $E_f$ . The incident  $h\nu$  energy photon, will creates the electron which has  $E_k^1$  energy relative to vacuum level,  $E_v$ .  $E_k$ , kinetic energy of electron which detected by analyzer will be counted by equation (2.1).

$$E_k = E_k^1 - (\Phi_{\text{spec}} - \Phi_s) \quad (2.1)$$

$\Phi_{\text{spec}}$  and  $\Phi_s$  are respectively spectrometer and specimen work function which is the amount energy that needs to excite electron from fermi level to the vacuum level. The Figure 2.9 which has electrical contact that the ejected photoelectron's binding energy from sample's kinetic energy will be counted by equation (2.2). That equation illustrates the photoelectron effect.

$$E_k = h\nu - E_b - \Phi_{\text{spec}} \quad (2.2)$$

Here  $h\nu$  is the incident photon energy,  $\Phi_{\text{spec}}$  is the photoelectron's work function of fermi level electron that required to excite electron to vacuum level.  $E_b$  is the binding energy shows the state relative to the fermi level.  $E_k$  is the kinetic energy that read by analyzer. Moreover, in the photoemission process after  $10^{-14}$  second the ejected photoelectron unoccupied electron will be occupied by upper orbital electron. During this transition, the emitted energy release either as X-ray or excites an above orbital electron. The excited electron is known as an Auger electron. The Auger electron energy is counted by equation (2.3).

$$E_k^{\text{auger}} = E_b^1 - E_b^2 - E_b^3 - \Phi_{\text{spec}} \quad (2.3)$$

$E_b^i$  shows the  $i$ th atomic level binding energy which is created by photoelectron.  $E_k^{\text{auger}}$  is emitted last electron's kinetic energy. The difference between Auger electron and photoelectron is that Auger electron's kinetic energy which does not depend on source energy while photoelectron kinetic energy depends on source energy. Auger electron kinetic energy depends on each elements' orbital level distinction. Therefore, Auger peaks are the characteristic peaks in the spectrum.

### 2.3.3. Surface Sensitivity of Photoemission

XPS, photoelectron process happens in the atom's core shell up to valence band. The XPS is not just occurred on the surface it is also can penetrate about micron range. However, due to inelastic scattering, the surface electron could reach the detector without losing their electron. Therefore, this makes the XPS as a surface sensitive analyzer.

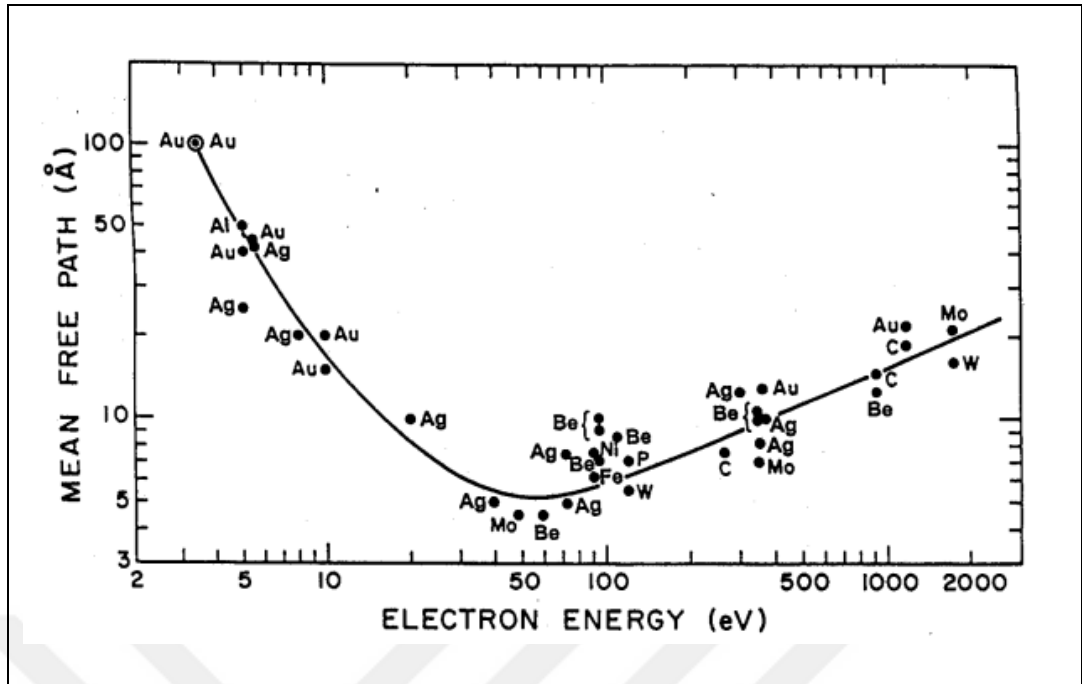


Figure 2.10: The mean free path of electrons in different solids as a function of electrons kinetic energy.

As it is mentioned above, the effect of inelastic scattering in XPS is very significant. For different materials, the inelastic mean free path (IMFP) depends on electron energy. IMFP curve which is mentioned in the Figure 2.10 [49] displays that the IMFP is that the electron's path without inelastic scattering in the solid. It depends on the electron's kinetic energy and materials. It can be seen that the IFMP is in the angstrom range, when the electron ejects from the sample traverse to the detector, it should be preserved from inelastic scattering, therefore, the XPS environment should be in the UHV condition to avoid electron's inelastic scattering.

Furthermore, the IMFP can be used to define the depth analysis from the electrons inelastic mean free paths [50]. The IMFP are also related to the atom size. Due to the restriction of the IMFP, XPS cannot penetrate in the sample get more knowledge in the deep layer element. XPS can go a few nm range. The IMFP plays an important role in surface physics. It is needed for quantitative surface analysis by AES and XPS and it helps to determine the surface sensitivity of photoemission experiment. The IMFP briefly is that the average of distances, measured along the trajectories that particles with a given energy travel between inelastic collision in a substance.

### 2.3.4. Experimental Technique

In general, the sample is bombarded with x-ray to eject electrons from the surface. This process can happen until, the amount of binding energy of electron less than the X-ray, then electrons are ejected. The ejected electrons are detected by analyzer, and the binding energy ( $E_b$ ) is computed by equation (2.4). An X-ray photoelectron spectrometer is shown as in 2D view, in Figure 2.5. Its essential components are; a specially constructed X-ray tube with a magnesium anode that produces a beam of the Mg Ka X-rays (1253.6 eV), and Aluminum anode that produces a beam of the Al Ka X-rays (1486.6 eV) ; an apparatus for exposing solid samples to the X-ray beam under a variety of conditions (cooled, heated, etc.); an electron multiplier detector (Specs HMA) for counting the focused electrons; a flexibly programmable current-control and data-recording system consisting of a computer and associated electronics with which the spectrum can be scanned automatically. Moreover, the mainly XPS source is created by applying the bias to tungsten to create thermal electron emission which accelerated to the Mg or Al anode, when electron hits the anode, the X-ray occurs. Which is focused on the sample. The angle between source and sample is  $54.7^\circ$ . The ejected electrons from the sample reaches to the analyzer chamber. By counting the electron number depends on their kinetic energy. By using the equation (2.4), the binding energy can be calculated. The reason why the binding energy is selected is that the characteristic of the element is related the binding energy of electron.

### 2.3.5. Surface Electronic Structure

The characterization of the sample as mentioned before it depends on binding energy, therefore, the count of electron is counted vs its binding energy. The binding energy depends on some other energy and their relation is mentioned in equation (2.4). In the equation  $E_b$  is the electron binding energy,  $E_k$  is the kinetic energy of photoelectron,  $E_{h\nu}$  is the energy of the exciting X-ray, and  $\Phi$  is the spectrometer work function, a constant for a given analyzer. The electron energy analyzer scans the kinetic energy spectrum to record the  $E_k$  values of the discrete photoelectron.  $E_b$  can



be calculated by using of the energy conservation equation which is determined in Equation 2.4.

$$E_b = E_{hv} - E_k - \Phi \quad (2.4)$$

The XPS source is restricted, therefore, it can scan a restricted region such as with magnesium radiation, it is convenient to study K levels of elements up to about  $Z = 10$ , L levels to about  $Z = 27$ , M levels to about  $Z = 57$ , and N levels through the transuranium elements [46].

### **2.3.5.1. Chemical Shifts**

Chemical shift is one of the significant feature that are very important to analyze the specimens. The chemical shift is also very crucial for the chemist to use XPS to probe the chemical shift in electrons binding energies. The binding energies of core-electrons are affected by the valence electrons and therefore by the chemical environment of the atom. The attraction of the nucleus for a core-electron is somewhat diminished by the presence of the outer electrons. If one of these valence electrons is removed, the amount of shielding is diminished, and the effective nuclear charge experienced by the core-electron increases, thereby it causes increasing in the electron binding energy. Therefore, in a simple sense the shifts of the photoelectron lines are an XP spectrum reflects the increase in binding energy as the oxidation state of the becomes more positive. In general, any parameter such as oxidation state, ligand electronegativity, coordination that affects the electron density about the atom is expected to result in a chemical shift in electron binding energy.

The exact binding energy of an electron depends not only upon the level from which photoemission is occurring, but also depends on; oxidation of atom and the chemical and physical environment. Changes in any of the situation gives rise to small shifts in the peak positions in the spectrum that is called chemical shifts.

This kind of shift can be seen in XPS due to the technique's high resolution and it is an electron process. These two features are based on XPS that gives the core level energies as discrete. Therefore, they make the XP spectrum readable and interpretable.

Moreover, chemical shifts have some unique property. Atoms of a higher positive oxidation state exhibit a higher binding energy due to the extra coulombic interaction between the photo-emitted electron and the ion core. This ability to discriminate between different oxidation states and chemical environments is one of the major strengths of the XPS technique. This feature will be more significant in our work. While growing the  $\text{Cr}_2\text{O}_3$ , the other chromium phases are also occurred. The chemical shift will be main feature that to deduce the chromium oxide phases. In practice, resolving atoms showing slightly different chemical shifts is limited. It is limited by the peak widths which are directed by a combination of factors; such as

- the intrinsic width of the initial level and the lifetime of the final state
- the line-width of the incident radiation which can be improved by X-ray monochromators.
- electron energy analyzer's resolving power.

In most cases, the second factor is the major contribution to the overall line width.

Furthermore, a major part of the strength of XPS as an analytical tool lies in the fact that chemical shifts can be observed for every element in the periodic chart except for hydrogen. Obviously, magnitudes of chemical shifts will vary from element to element, and the sensitivity for a particular element will vary with the photoelectric cross section.

In the case of solid compounds, it is more difficult to write a chemical reaction having an energy equal to a given difference in binding energy, and more approximations must be made. However, the method has been successfully applied to the correlation of binding energies for solid compounds of nitrogen, boron, carbon, and iodine. The principal difficulty with the application of the "principle of equivalent cores" is that the necessary thermodynamic data are often lacking. Therefore, there is a need for a good general method for estimating differences in the heats of formation for pairs of isoelectronic species. A very crude method of this type, based on Pauling's concept of electronegativity, has been devised and successfully applied to the calculation of relative carbon 1s binding energies for a wide variety of organic compounds." It has also been shown that the core electron binding energy for an atom in a molecule is calculable as the sum of parameters,  $p_i$ , characteristic of the atoms or groups directly bonded to the atom from which the electron is ejected:  $E_b = \sum p_i$ .

These parameters can be evaluated empirically from experimental binding energies and used to predict unknown binding energies. The Figure 2.11 [51] illustrates the chemical shifts of carbon. It shows how carbon 1s binding energy changes with its different compounds.

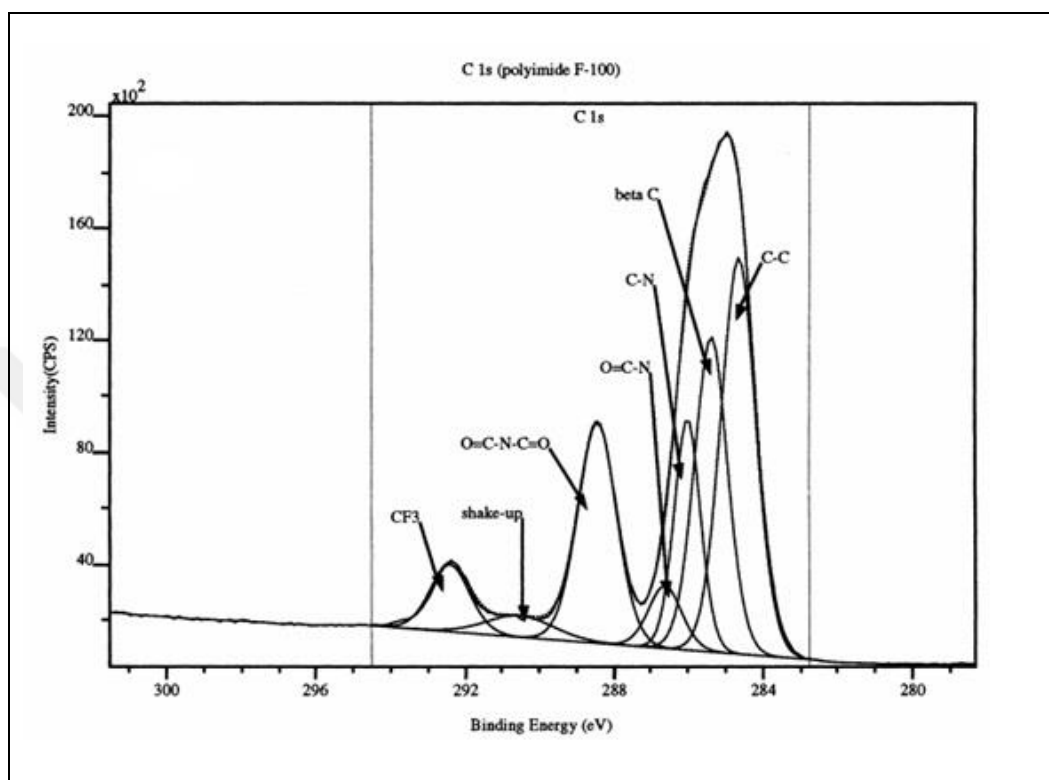


Figure 2.11: Chemical shift of C1s for different chemical bonding.

### 2.3.5.2. Level Splitting

One of the features to be displayed on the spectrum is Level Splitting. An interesting application of photoelectron spectroscopy is the study of splitting of atomic levels that are normally degenerate. The novel feature of this splitting is that it occurs in inner atomic core levels that are not accessible to study by classical techniques. The ejection of a photoelectron from a filled shell creates a hole in that shell, and the splitting can be thought of as arising from the interaction of the final-state electron hole with the electronic environment of the atom. Two types of splitting have been observed, which may be characterized as electrostatic splitting and magnetic, or exchange splitting.

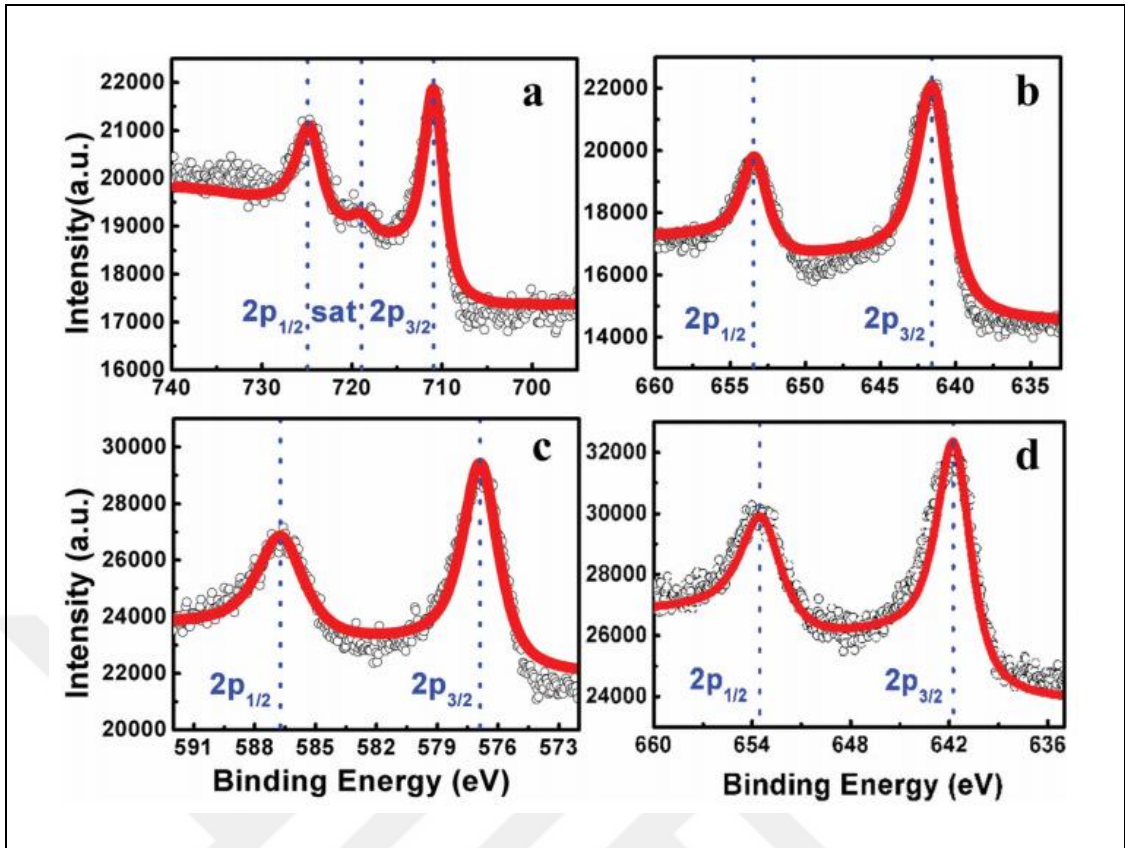


Figure 2.12: The exchange splitting of a) Fe2p, b) Mn2p for YFMO and c) Cr2p, d) Mn2p for YCMO.

Figure 2.12 [52] illustrates the exchange splitting of the Fe, Mn and Cr 2p peaks. This splitting is very clear that as it is displayed in Figure 2.12 that can help to define the phases. There are some properties that have effects on splitting. The splitting can be due to the two reasons:

- Electrostatic splitting

A study of heavy-element photoemission spectra has revealed a complex structure of photolines from  $5p_{3/2}$ , core levels. The splitting energy ranged from 3 to 10 eV in various compounds. These splittings were interpreted as arising from the differential interaction of the internal electrostatic field with the  $M = \pm 1/2$  and  $M = \pm 1/3$  substrates of the  $5p_{3/2}$ , electron.

- Exchange Splitting

The reason is due to the exchange splitting. The splitting comes from of the fact that, in a system with unpaired valence electrons, the exchange interaction affects core

electrons with spin up and spin down differently. The free atom model predicts also that the relative intensities of the two lines are simply the statistical weights of the two final states. The final-state spin ( $J$ ) gives the ratio of  $2J+1$  for the intensities of the two lines. Exchange splitting, taking the example of the emission of a core s electron from the  $Mn^{2+}$  ion, which has five unpaired d electrons, the final-state spin ( $J$ ) can be  $5/2 \pm 1/2$  and the intensities of the two lines would be expected to be in the ratio  $2J+1$ , or 7:5 as it can be seen in Figure 2.12 especially Figure 2.12 b) illustrate the Mn 2p exchange splitting.

## 2.3.6. Chemical and Elemental Composition of Surface

### 2.3.6.1. Quantitative Analysis

In the XPS work, specimen's chemical bond is very significant and also their concentration too. Both concentration and bond are counted by their ratio in the spectrum. This ratio is calculated from peak width and height and atomic sensitive factor. For a certain peak in the spectrum, for a homogeneous sample, its electrons are counted per second according to the in the equation (2.5),

$$I = n \cdot f \cdot \sigma \cdot \theta \cdot y \cdot \lambda \cdot A \cdot T \quad (2.5)$$

where,  $n$  is the number atom per volume ( $cm^3$ ),  $f$ , x-ray flow (photon/ $cm^2$ -s),  $\sigma$  is the atomic orbital photoelectron effect area ( $cm^2$ ),  $\theta$  is the angle between incident light and detected electron direction,  $y$  is the efficiency that depends on the photoelectron energy,  $\lambda$  is the IMFP of the specimen electron,  $A$  is the specimen area and  $T$  is the efficiency of the detected electron. From the equation (2.6) the number of electron per unit volume is counted. The denominator is named atomic sensitive factor (ASF),  $S$ .

$$N = \frac{1}{f \cdot \sigma \cdot \theta \cdot y \cdot \lambda \cdot A \cdot T} \quad (2.6)$$

As it is aforementioned, the specimen element analysis counted by the ratio of the elements. And it is given by the equation of (2.7).

$$\frac{n_1}{n_2} = \frac{I_1/S_1}{I_2/S_2} \quad (2.7)$$

$I_1$  and  $I_2$  are 1<sup>st</sup> and 2<sup>nd</sup> element's main peak area which gives photoelectron intensity.  $S_1$  and  $S_2$  are the 1<sup>st</sup> and 2<sup>nd</sup> elements orbital levels atomic sensitive factor. If the  $S_1/S_2$  ratio is independent from the materials, it can be used for the all homogeny materials. Even  $\sigma$  and  $\lambda$  have different values for different materials,  $\sigma_1/\sigma_2$  and  $\lambda_1/\lambda_2$  ratios are almost constant, therefore, in any spectrum the ASF can be calculated.

$$C_x = \frac{n_x}{\sum_i n_i} = \frac{I_x/S_x}{\sum_i I_i/S_i} \quad (2.8)$$

$C_x$  is the concentration of an x element. For different core levels and from their ASF, the intensity will be found. So the atomic concentration can be calculated by using the equation (2.8). This equation is valuable if the sample surface is homogenous. If the surface is not homogenous, the sample structure model should be known.

Shake up is one of the significant peak that can be seen on the spectrum. It is very important feature for elemental analysis. It needs to be named the peak correctly whether it is a photoelectron from core level or inelastic scattering electron. The shake up occurs when the electrons interacts with a valence electron and excites it to a higher energy level. As a result, the energy core electron in the photoemission process appears to increase the nuclear charge. This fact leads to substantial reorganization of the valence electrons, in other words relaxation, which may involve excitation of one electron to a higher unfilled level that is called shake-up. This two-electron process leads to a discrete structure on the higher binding energy side of the photoelectron peak a shake-up satellite. The shake up peaks of the Cu can be seen in the Figure 2.13 [53].

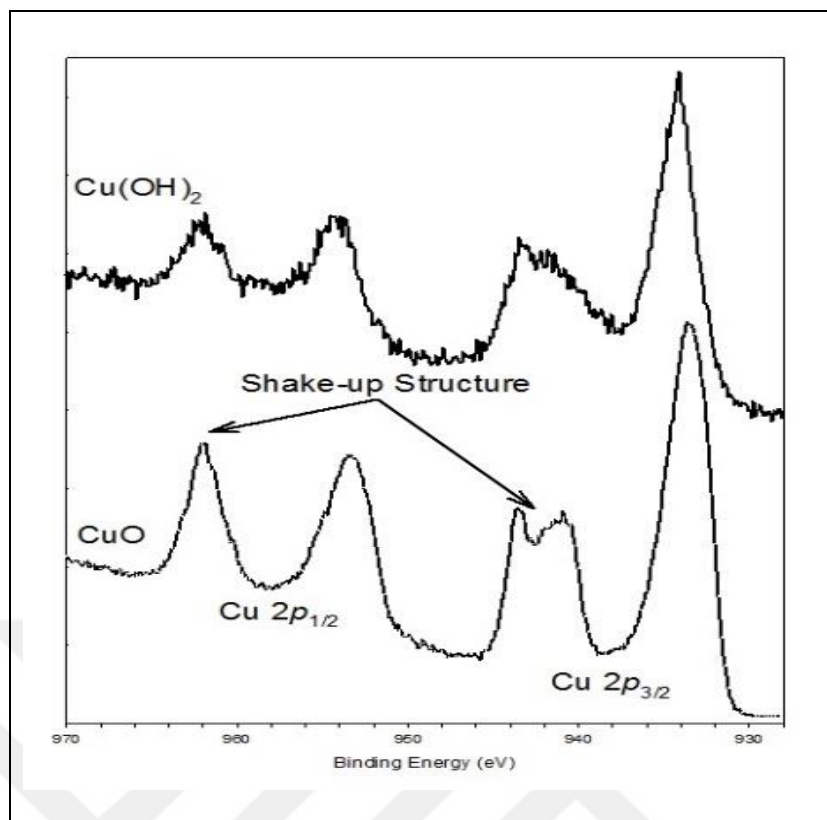


Figure 2.13: The shake-up satellite peak of the Cu.

Another feature can be seen on the XP spectrum is plasmons which are created by collective excitations of the valence band. There are two type of plasmons. One of them is Extrinsic Plasmon that is due to the excited as the energetic PE propagates through the solid after the photoelectric process. The other one is Intrinsic Plasmon which is screening response of the solid to the sudden creation of the core hole in one of its atom. Briefly, the plasmon is occurred when the photoelectron excites collective oscillations in the conduction band (free electron gas), so called Plasmons (discrete energy loss). In Figure 2.14 [40] illustrates the plasmon peak of Al.

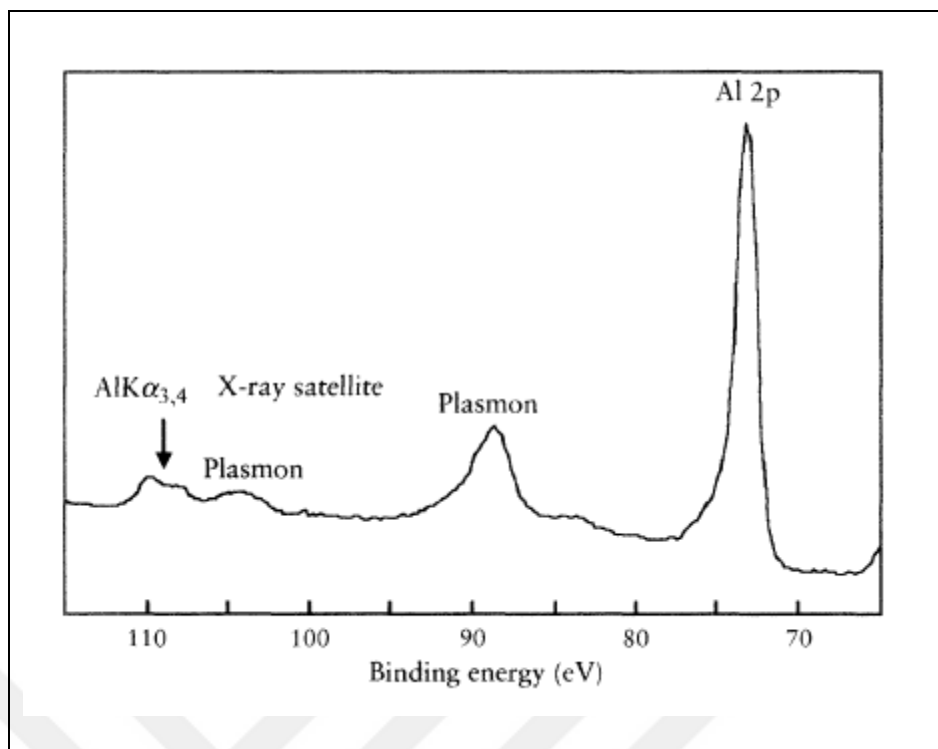


Figure 2.14: Plasmon loss features from clean Aluminum.

Another peak that can be seen on the spectrum is shake-off. In the process similar to shake-up valence electrons can be completely ionized and extracted from an atom to an unbounded continuum state. Such a process is called “shake-off” and leaves an ion with vacancies in both the core level and a valence zone. Discrete shake-off satellites are not to be seen in XPS of solids. The shake-off satellites tend to appear within the region of the broad inelastic background and transitions from discrete levels to a continuum produce broad shoulders of core level peaks rather than separate peaks.

All the above statements define the nature of the XPS and its data. However, the raw data would not help to do quantitative analysis. The raw data of XP spectrum consists of background noise. Therefore, this background noise should be removed from the spectrum. There are several methods have been used for background removing. Such as Shirley, Seah, Tougaard.



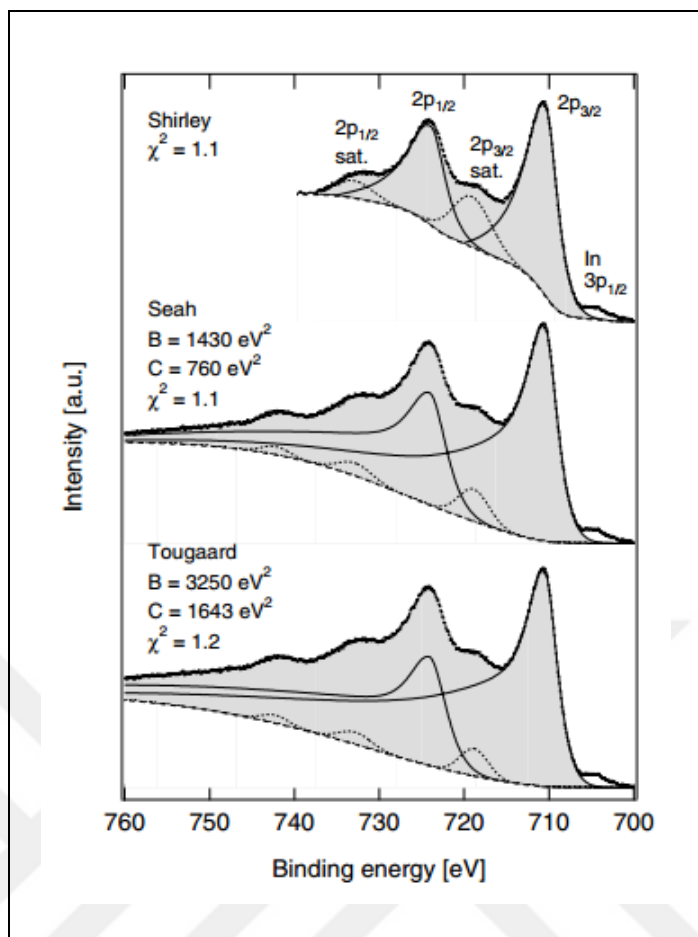


Figure 2.15: Curve fits to the Fe2p region of the reference sample after applying three different background subtraction methods. The main peaks are drawn with a solid line, the shake-up satellites with a dotted line, and the background with a dashed line. The shaded area indicates the sum of the component peaks.

As it can be seen in Figure 2.15 [54], the background subtraction methods have a significant effect on spectrum. After applying background subtraction methods, the spectrum feature might be changed. Therefore, while employing any background subtraction methods, should be very careful. Any wrong feature would cause misinterpret of the peak.

After background subtraction, then the spectrum needs to be fitted. As it can be seen in Figure 2.16 [55], the Lorentzian, Gaussian, and Voigt functions are applied. The Voigt function is the convolution of Lorentzian and Gaussian functions. In this work, Voigt has been used to do fit of the peak.

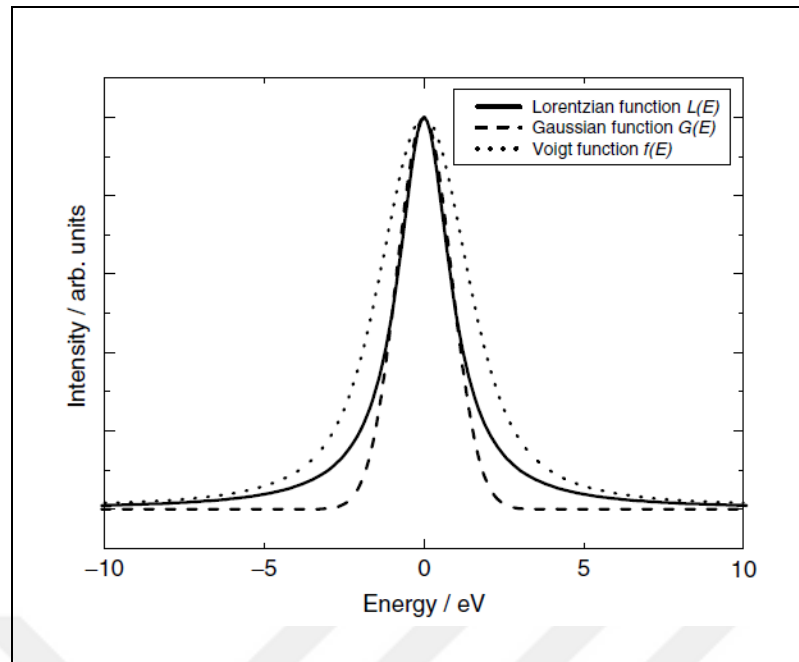


Figure 2.16: Comparison of a Gaussian and a Lorentzian function with FWHM = 2 eV with the result of the convolution of both, the Voigt function.

In conclusion, the XPS is very wide range applicable methods to characterize the thin films that give the elemental analysis and their ratio. Therefore, their chemical structure can be defined. XPS can be used for analysis of all elements in the periodic table except hydrogen and helium. The hydrogen cannot be detected just because of the hydrogen has only one electron. The Helium cannot be detected because of the detection level of it is under the background level of the XPS. While X-rays interact only weakly with matter and consequently can penetrate deeply into a solid (10 nm), electrons with energy in the range 5-1500 eV readily lose energy by inelastic scattering.

### **3. GROWTH of FILMS STABLE of CHROMIUM OXIDE THIN FILMS**

In this section, the results of the growth of the chromium oxide on naturally oxide silicon single crystal by Pulsed DC and RF magnetron sputtering are going to be presented. The parameters of both methods were optimized for chromium oxide growth such as growth temperature, post annealing temperature which is applied mostly after the growth of the sample completed, bias voltages, and differential pressure of argon-oxygen gases. The optimized parameter will be used for future works like as multilayer films applications. Substrate temperature, differential pressure of gases are very crucial parameters that have very significant effect on thin film growth [42].

As first step, the Si crystal used as substrate was cleaned before mounted on the sample holder. After cleaning process to prepare for UHV conditions, the substrates are transferred to the load-lock chamber. The samples were kept in Load-Lock under HV conditions during the study. The depositions chamber has UVH vacuum condition ( $>10^{-9}$  mbar) as base pressure. For the deposition, the sample holder with Si substrate is transferred to the sample manipulator in the magnetron deposition chamber. The manipulator can move under the 6 magnetron guns and it has capability to anneal the sample up to  $1500^{\circ}\text{C}$  during deposition or after deposition. It heats via radiation is provided by PBN Heater. It works up to  $<10^{-5}$  mbarr partial oxygen pressure. For deposition, the plasma is made by releasing Ar gas and applying power on Magnetron Gun so that the vacuum level might decrease to  $2 \times 10^{-3}$  mbarr. To obtain oxide film, oxygen is needed to feed the chamber in certain level. By applying bias to the Cr target to obtain plasma with Ar, and ionized Ar atoms in plasma wear off the small fragments from the target surface. Meanwhile the oxygen leaks into the chamber during plasma existing. The mix ratio of Argon and Oxygen gas is another parameter to grow Cr-Oxide films during reactive deposition. After the completing of deposition process, the samples on the holder are transferred to the Analytical chamber over the load-lock. One of strong surface photoemission spectroscopic technique is XPS and it was used to define oxidation level in the Cr-Oxide films. XPS is a very sensitive for surface characterization. It gives the element and their chemical composition in atomic level.

### **3.1. Preparation of Substrate Silicon Single Crystal (100) Towards Film Growth by Magnetron Sputtering in UHV Conditions**

The main goal is to grow the  $\text{Cr}_2\text{O}_3$  thin film by magnetron sputtering on silicon single crystal (100). The silicon single crystal is polished. To grow the thin film, initially it needs a very well defined surface, because the substrate surface affects much to the growth of thin film [29]. In this work, therefore, the well-known naturally oxide silicon single crystal has been prepared. Even it is polished, it is not totally cleaned enough for UHV conditions because the atmospheric conditions cause some surface contaminations so that they came out from the surface in UHV conditions such as water molecules, some hydrocarbons type fragments. In order to remove that contaminations, the cleaning process has been done in a couple of steps. In first step, the silicon substrates pieces are cleaned with ethanol in ultrasonic bath for 5 minutes. And after being taken out, Si substrates are flashed with ethanol; then they are mounted to the holder as it is shown in Figure 3.1. The substrate is cleaned ultrasonically, are mounted to the sample holders and transferred in to the load-lock. The load-lock can have almost 10 sample holders and it is localized between the deposition chamber and analytical chambers. After loading process is done, in order to hold vacuum in the load-lock the vacuum pump system is started while the glass gate door on the load-lock is closed. The vacuum of the load-lock chamber can reach up ultimately to  $<2 \times 10^{-8}$  mbar in 24 hours which is assumed HV level. When the load lock vacuum reaches upper level which is HV, it means that it is ready to transport the samples to the magnetron sputtering chamber for growth. Otherwise, when the load lock pressure is very high it would contaminate the chamber over long time period. The contaminated chamber always affects the film quality. It is also observable by photoemission spectrums in analytical chambers. And those contaminations will show in the spectra. That is the waste of the energy and time. To avoid these problems, we need to be more careful during cleaning and loading processes of substrates. When the growth is completed, the sample is transferred to the load lock without expose to the atmospheric conditions. It keeps the sample's surface clean and then the sample is taken in to the analytical chamber in order to proceed the surface chemical analyzing by the XPS. Since the load lock has a capability of storage up to 10 samples, it creates possibility to prepare the multiple samples one loading time; therefore, there is no need to prepare

the substrates for every times. Mostly, after the substrates cleaned in atmospheric conditions are transported to the deposition chamber one more cleaning step via annealing up to 500°C to remove any trace amount of residual contamination on the surface of the substrates. Then the growth process starts. There are three possible growth processes in the Magnetron sputtering chamber: DC, Pulsed DC and RF Magnetron Sputtering. It is well-known that DC-magnetron sputtering has some restrictions. If reactive gas is used with Argon-Process gas to make oxide films, the target loaded metals such as Cr is easily poisoned and the deposition rate decreased dramatically. During growth of the any oxidized sample, after a while, the target either oxidized or charge accumulation on the target surface cause of the decreasing of the growth rate; even the DC Magnetron Sputtering deposition rate is faster than the Pulsed DC and RF Magnetron Sputtering. Therefore, in this study, experiments are done with Pulsed DC and RF magnetron sputtering. After the growth of Cr<sub>2</sub>O<sub>3</sub> thin film is optimized with Pulsed DC Magnetron Sputtering, the Cr<sub>2</sub>O<sub>3</sub> thin film growth parameter has been optimized for RF Magnetron Sputtering. The growth thickness is controlled in-situ real time by the QCM and the surface elemental analysis by XPS. Also, QCM parameters is calibrated by photoemission attenuation study in order to increase the thickness reading sensitivity in the range of 0.1 Å/sec.



Figure 3.1: Specimen and sample holder.

### 3.2. Cr<sub>2</sub>O<sub>3</sub> Growth on Si Crystal by Pulsed DC Magnetron Sputtering

In this part, the growth of Cr oxide thin film by Pulsed DC magnetron sputtering will be discussed. While DC magnetron sputtering can cause target poisoning, Pulsed DC vibrates the plasma with 100 kHz so that the reactive plasma hit and release on the surface of target 100k times in second; and it results decreasing target poisoning but this decrement wears the particles from the surface.

Initially, Cr<sub>2</sub>O<sub>3</sub> phase has been obtained with optimized parameters such as plasma power and partial pressure of plasma. The results of growth with Pulsed DC will be discussed in the following pages. In the literature, the growth has been done with different substrates temperature and oxygen and argon flow rate. In this work, naturally oxide Si single crystal is used as a substrate, main purpose was to obtain Cr<sub>2</sub>O<sub>3</sub> phase with lowest temperature. The work started from low temperature to high temperature until to get optimized Cr<sub>2</sub>O<sub>3</sub> phase. To understand each of parameters effects on specimens, the samples growth is analyzed by using XPS to search out Cr<sub>2</sub>O<sub>3</sub> phases. It is purpose that the Cr<sub>2</sub>O<sub>3</sub> films growth will be used as an antiferromagnetic layer in multilayers films device; therefore, the optimized parameter must be well-defined to develop reproducible oxide film. According Huggins, C. P. et al, the lowest substrate temperature Cr<sub>2</sub>O<sub>3</sub> phase has been gotten at 400 °C. [56]. In addition, one of the work succeeded Cr<sub>2</sub>O<sub>3</sub> phases above about 280°C; in that temperature, the CrO<sub>2</sub> decomposes to the most stable oxide of chromium, Cr<sub>2</sub>O<sub>3</sub> [6]. This behavior of temperature also can be seen in this study.

It is trivial that the temperature such as post annealing and annealing affect the growth process of Cr<sub>2</sub>O<sub>3</sub> phases. That's why, some of the post annealing and annealing temperatures have been performed to understand how the growth mechanism develops with different temperature application. The annealing is employed the sample while growth and the post annealing is employed after the growth process has been completed.

Initially, the specimen P0 is prepared as the pure Cr films was grown on the substrate. The thickness is 480 Å in order to bury the peak of photoemission coming from the substrate. As it is shown in Figure 3.2 the Cr is coated on naturally oxidized silicon crystal with Pulsed DC. The Cr 2p<sub>3/2</sub> peak is 574.3 eV. This photo emission spectrum is used as a reference of pure Cr surface to the Cr-Oxide surfaces. That is

comparable to the value which is published in literature [57]-[60]. Such as according to H. Ma, shows the binding energy of metallic Cr at 574.2 eV [58].

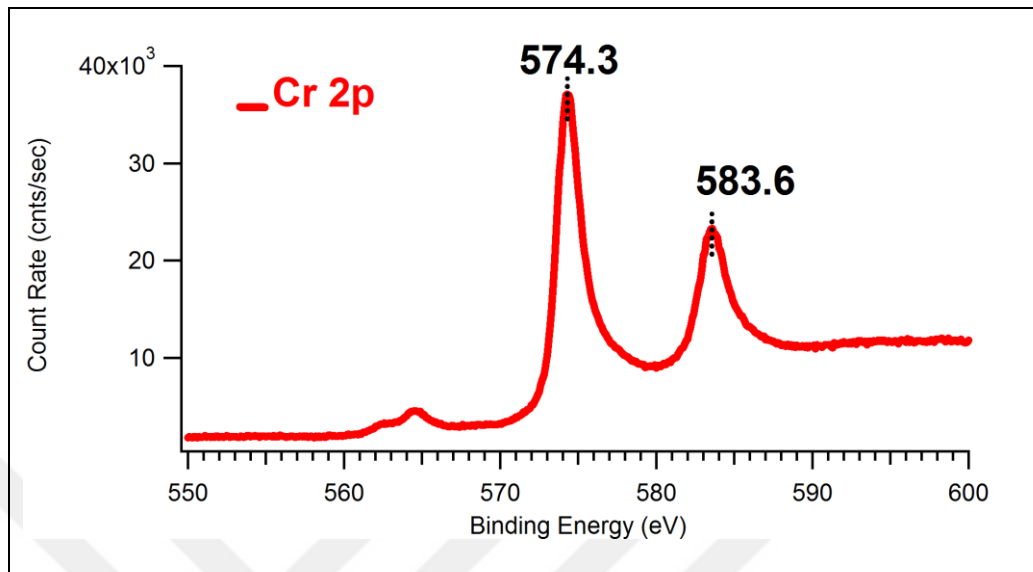


Figure 3.2: The spectrum of Cr growth on naturally oxidized silicon crystal (100). The growth has been done by Pulsed DC at RT for 428 Å for P0 specimen.

According to Huggins, C. P., the spin-orbit splitting changed from 9.2 eV to 9.7 eV [43]. As it can be seen from the Figure 3.2 for the specimen P0, the spin orbit-splitting for pure chromium metal changed is 9.3 eV. And also it is going to be seen in the following parts that the Cr oxide thin film shows the spin-orbit splitting changed from 9.6 eV to 9.9 eV. It is also indication of oxidation level on the Cr-Oxide surfaces.

In the following paragraphs, it will explain extensively the growth of Cr<sub>2</sub>O<sub>3</sub> thin films have been done with Pulsed DC magnetron sputtering and analysis of this films by XPS. Before starting the growth, the pure Cr target was applied 100 V while the chamber was fed by argon gas for 5 minutes.

Initial growth of the Cr-oxide has been done under UHV condition which has a base pressure of  $\sim 10^{-9}$  mbar with Pulsed DC Magnetron Sputtering at room temperature (RT) with different oxygen flows, such as 0.2, 0.23, 0.3 sccm. The different oxygen flows have been performed because in literature the effect of the oxygen pressure was observed clearly [56]. Meanwhile the argon pressure is kept at 3 sccm during all different oxygen flows. As it seen in the Figure 3.3, the 0.3 sccm Argon gas feed with 0.2 sccm Oxygen gas for the sample P1\_1, 0.23 sccm Oxygen gas for the for the sample P1\_2 and 0.3 Oxygen gas for the sample P1\_3.

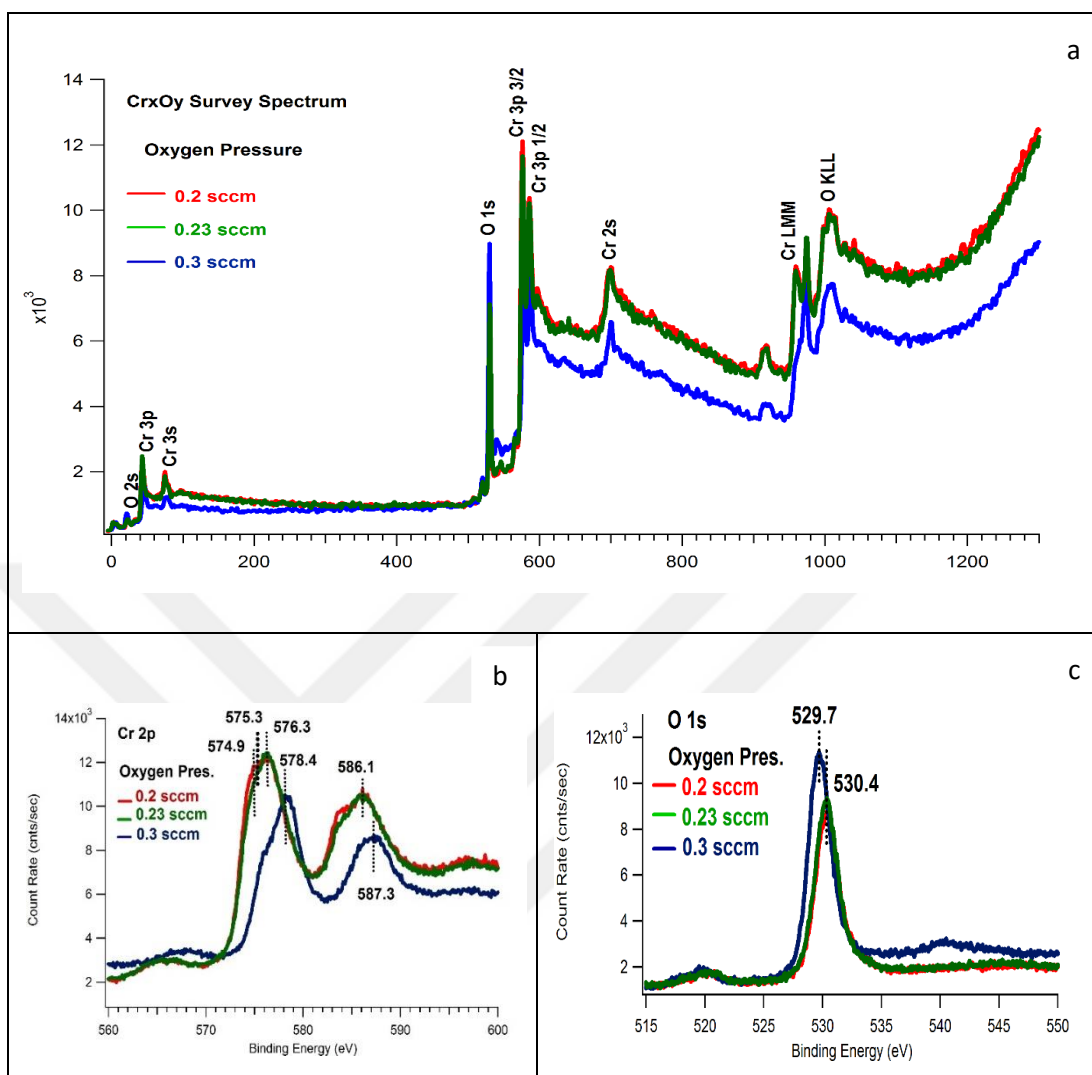


Figure 3.3: The growth of  $\text{Cr}_2\text{O}_3$  is performed under 0.3 sccm Argon gas and for 0.2, 0.23, 0.3 sccm Oxygen gas XPS spectrum. a) survey XP spectrum b)  $\text{Cr}2p_{3/2}$  XP spectrum c)  $\text{O}1s$  XP spectrum for P1\_1, P1\_2, P1\_3.

These samples are going to be first step of this study. The optimized parameters will be the next step. When the oxygen flow rate was 0.2 and 0.23 sccm for P1\_1 and P1\_2 samples have 150 Å thickness. However, the when the differential oxygen pressure was 0.3 sccm the thickness was 39 Å. After around 40 minutes, the QCM could not read any flow rate. Therefore, the following studies has been done for 0.23 sccm for oxygen.



Table 3.1: The Cr growth on Si crystal with Pulsed DC Magnetron Sputtering in UHV condition at RT for 3 sccm Argon pressure and for 0.23 and 0.3 sccm oxygen pressure Cr phases peaks.

Cr <sub>2p3/2</sub>	Literature	P1_1	P1_2	P1_3
Cr	574.2 eV A. Maetaki [58]	574.9 (eV)		
Cr <sup>3+</sup>	577 eV A. Maetaki [58]			
Cr <sup>4+</sup>	576 eV A. Maetaki [58]	576.3 (eV)	575.3-576.3 (eV)	575.8 (eV)
Cr <sup>6+</sup>	579 eV K. Asami [61]			578.4 (eV)

The gas pressure shows the clear effect on the Cr-oxide phases as it can be seen in Table 3.1. And the main peak is matched with the literature work. During this process, the power of magnetron gun was kept at 20W. It is observed that the partial gas pressure has a distinct effect on the metal oxide thin film growth. The gas flows of 0.3 sccm and 0.23 sccm for Argon and Oxygen in respectively, shows more dominant Cr<sub>2</sub>O<sub>3</sub> peak relatively compare to other oxygen partial pressure performances. This spectrum shows that the Cr<sub>2</sub>O<sub>3</sub> is seen, from the peak of Cr<sub>2p3/2</sub> that the BE is 576.3 eV. Generally, in the literature, the binding energy of Cr (III) is between 576 and 577 eV. Such as K. Asami [61] showed the Cr (III) 2p BE is 576.7 eV. On the other hand, A. Maetaki [58] displayed the Cr (III) 2p<sub>3/2</sub> BE is 577 eV. The pure Chromium 2p 3/2 peak BE is at 574.9 eV. At the 575.8 eV spectrum is Cr (IV). As it can be seen in Figure 3.3, the low oxygen sccm Cr<sub>2p</sub> has wide peak instead a narrow compare to the 0.23 sccm. While the other parameters are kept constant, just changing the oxygen partial pressure to the 0.3 sccm, the Cr<sub>2p3/2</sub> peak 1.8 eV shifts. In this case the Cr<sub>2p3/2</sub> peak is displayed the BE at 579 eV is the Cr (VI) phase. These peak shifts are summarized in Table 3.1 above. Therefore, in this case, higher sccm oxygen is not wanted.

The growth has been done under room temperature so far. Moreover, from the spectrum, it can be seen that it does not just show the Cr<sub>2</sub>O<sub>3</sub> peak. There are also other peaks which can be seen on the spectrum. Consequently, the other parameter has been also changed to get a best phase of Cr<sub>2</sub>O<sub>3</sub>. It is known that there are always impurities

coming from other oxide phases even the most is  $\text{Cr}_2\text{O}_3$ . As long as the sensitivity of photo emission allows the purities level of  $\text{Cr}_2\text{O}_3$  will be get better.

After optimized oxygen flows rate, the substrate temperature has been changed to probe the substrate temperature effect on Cr phases. The substrate temperature is changed from RT to the  $300^\circ\text{C}$  by  $50^\circ\text{C}$  increments. Those peaks have been plotted as in the below Figure 3.4.

In this step, the best gas partial pressure observed so far has been taken constant, and the substrate temperature was also kept at RT. The changes were made for post annealing. The feeding of the gases which were 0.23 sccm for oxygen, 3 sccm for Argon and the substrate was at RT. The thickness of  $\text{Cr}_2\text{O}_3$  was  $151 \text{ \AA}$ . Each time the sample post annealed for 20 minutes. After each temperature the spectrum has been taken to see the difference. As it can be seen from the Figure 3.4, the binding energy of the Cr2p and O1s phases are increase by the temperature increment.

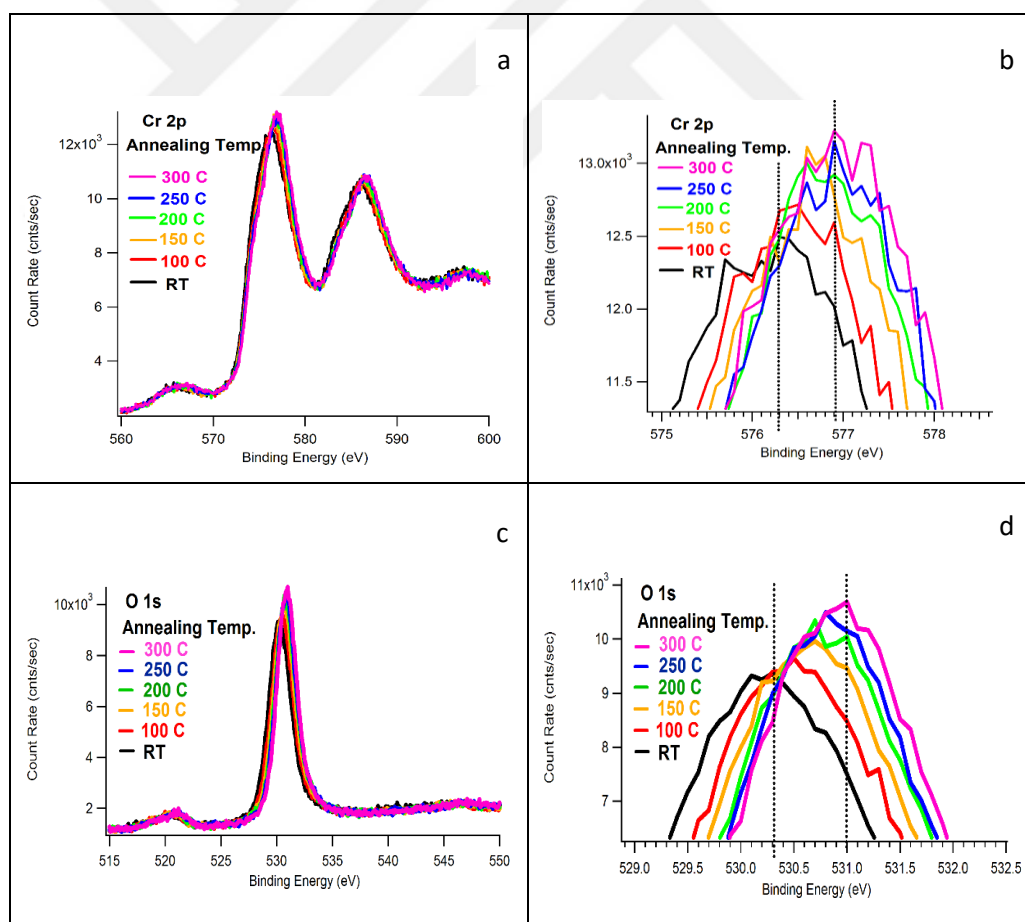


Figure 3.4: The XPS of RT substrate growth of  $\text{Cr}_2\text{O}_3$  and the sample was annealed from RT to  $300^\circ\text{C}$ . a) and b) display the Cr2p spectrum peak. c) and d) shows the O1s peak of the P2 specimen.

The P2 sample has been deposited at RT. Then it was post annealed from 100°C to 300°C in order to analyze the post annealing effect on the Cr phases. Thickness of the P2 is 151 Å. The post annealing has been employed for each temperature for 20 minutes.

Table 3.2 The XPS of RT substrate growth of Cr on Si crystal and the sample was annealed for RT to 300°C.

Cr2p 3/2	Main Peak(eV)	Cr Phases
RT	576.3	576 eV A. Maetaki [58]
100°C	576.4	
150°C	576.6	
200°C	576.6	
250°C	576.9	
300°C	576.9	577 eV A. Maetaki [58]

At the room temperature the main peak of the Cr2p<sub>3/2</sub> has two peaks which are at the 575.6 eV and 576.3 eV, in this range, it belongs to the Cr (IV) binding energy. When annealed at 100°C, the shoulder at the 575.6 eV has disappeared. The peak at 576.3 eV got narrow. Still there is no Cr (III). After annealing at 150°C, the main peak shift to the 575.5 eV and it has shoulder at 576.6 eV, (576.6 eV binding energy is from the Cr (III)), which shows that the process is correct. But the Cr (III) peak is not dominant. When the sample is annealed at 200°C, the spectrum shows that the main peak of Cr2p stays in the same position as 150°C does. As it can be seen for annealed at 250°C and 300°C, the main peak is at the 576.9 eV. That is the Cr (III) peak. Table 3.2 shows all peaks shifts on the XPS graphs. It can be said from the XPS spectra, the Cr<sub>2</sub>O<sub>3</sub> get more dominant at the higher temperatures. The XPS graphs show that the thin film consists of Cr<sub>2</sub>O<sub>3</sub>, but the other Cr phases present in the oxide films surface. After first try, second part has been performed under the same bias, 20 W. After figuring out the importance of the post annealing. And it still having shoulder. Next step is going to be about growth of the samples for variety substrate temperature and post annealing.

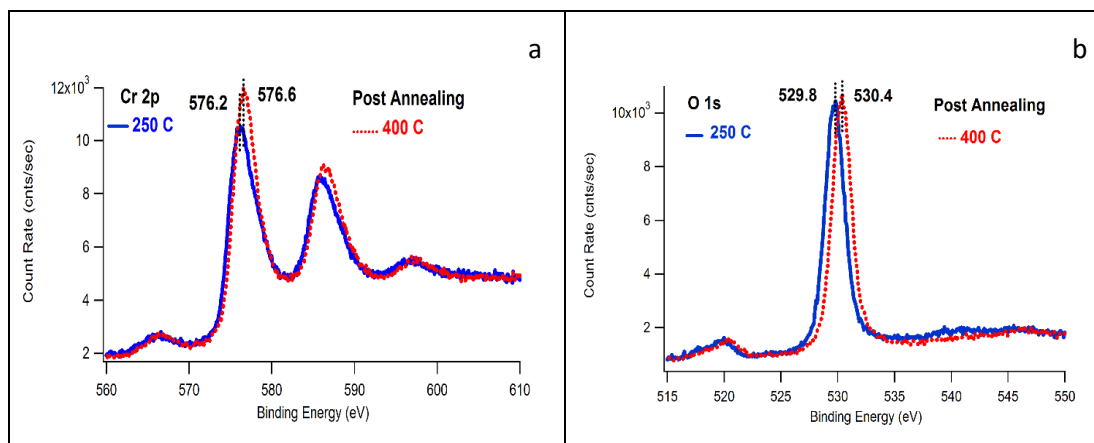


Figure 3.5: The XPS result of  $\text{Cr}_2\text{O}_3$  growth at 20 W and substrate  $250^\circ\text{C}$  and then the sample was employed post annealing at  $400^\circ\text{C}$ . a) Cr2p and b) O1s spectra for P3 specimen.

While growing the sample at the RT, the desired phase didn't form. The gases partial pressure kept same value such as MFC for oxygen was 0.23 sccm and argon 3 sccm. In this step, the growth has been done at  $250^\circ\text{C}$  substrate temperature. In Figure 3.5, the XPS data from the sample growth at the  $250^\circ\text{C}$  substrate temperature shows the peaks for Cr  $2p_{3/2}$  at 576.2 eV, which is appropriate to Cr (IV)-oxide phase. The changing the substrate temperature does not affect much to the growth of  $\text{Cr}_2\text{O}_3$ . Therefore, the post annealed applied to the sample since it is known from previous work that it has some effect on the growth of oxide film directly. This time, the sample annealed at  $400^\circ\text{C}$ , and the Cr (III) peak of  $2p_{3/2}$  BE presents at 576.6 eV as shown in Figure 3.5. After annealing, it can be seen that there is a shift, in the main peak, which is equivalent to 0.4 eV. Still there is feature shown as a shoulder due to the other Cr phases. However, the Cr (III) is very dominant than other peaks. This result is much promising and reasonably acceptable result comparing to of  $\text{Cr}_2\text{O}_3$  growth observed in the literature, since it is well known that Pulsed DC magnetron deposition has some limited capabilities while growing metal oxide thin films. It is not like DC Magnetron which has target poisoning, Pulsed DC technique might show some problem especially in slow growing proses. In the beginning of the deposition, the deposition rates were 0.3 and 0.4  $\text{\AA}/\text{s}$ . When the sample growth reaches to the 81  $\text{\AA}$ , the deposition rate decreased to the 0.2  $\text{\AA}/\text{s}$ . gradually, the rate of deposition went zero after the sample reach 112  $\text{\AA}$ . The thickness of the sample is 114  $\text{\AA}$ , and it is obtained for 450 second. This degradation on deposition rate indicates the poisoning of Cr-target during Pulsed DC deposition.

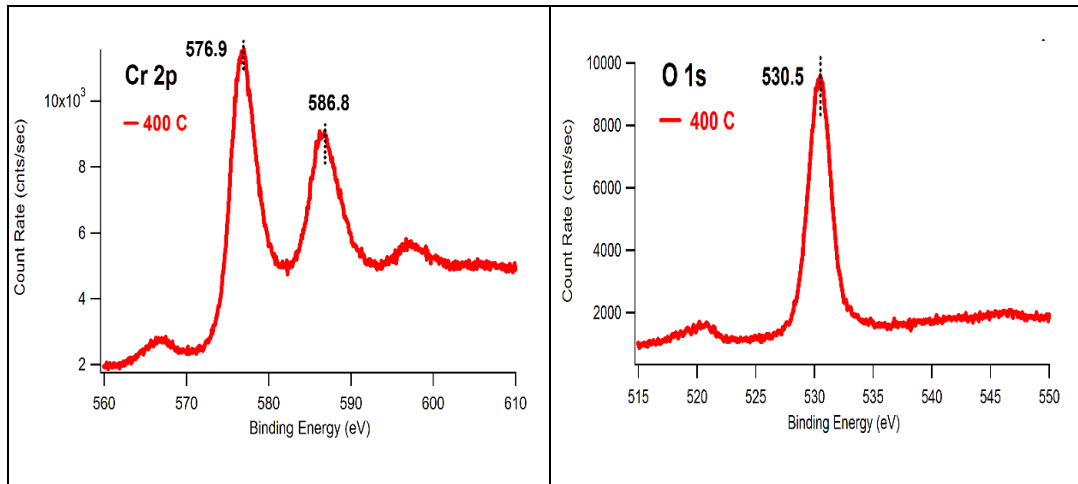


Figure 3.6: The growth of  $\text{Cr}_2\text{O}_3$  at  $400^\circ\text{C}$  substrate, 20 W, MFC of oxygen is 0.23 sccm and argon is 3 sccm. a) Cr2p b) O1s XPS spectrum for P4 specimen.

Even before growth of the P4 sample, the target was cleaned by applying 100 V for 300 second after a while target got poisoned. Then the deposition stopped. As observed during Pulsed DC depositions, the higher post annealing temperature results increasing the existence of  $\text{Cr}_2\text{O}_3$  phase in the oxide films. The post annealing temperature at  $400^\circ\text{C}$  gave a better result. The main of  $\text{Cr}2p_{3/2}$  is at the 576.9 eV which belongs to that Cr (III). The P4 sample, the thickness is  $99 \text{ \AA}$ , and the deposition rate was between 0.3 and  $0.4 \text{ \AA/s}$ . While starting the growth, the surface of the pure Chromium surface oxidized, therefore, the ratio of removed chromium atom decreases. Due to the restriction of the Pulsed DC magnetron sputtering, we had to change to the RF magnetron sputtering for obtaining to get the good result as expected the thick of the thin film.

### 3.3. $\text{Cr}_2\text{O}_3$ Growth on Si Crystal by RF Magnetron Sputtering

The Pulsed DC magnetron sputtering deposition has succeeded limitedly to grow  $\text{Cr}_2\text{O}_3$  since for the long period deposition it has failed. The deposition rate decreases with respect of oxygen flow rate and the existence of oxygen poisons on Pure Chromium Target. Typically, the higher power used to make the plasma and the higher oxygen rate increase oxygen poisoning on the target. Due to that restriction, RF magnetron sputtering deposition technique is experimented to grow  $\text{Cr}_2\text{O}_3$ .

At the beginning, the parameters optimized for Pulsed DC Depositions were used for RF Magnetron Deposition. As it can be seen from the Figure. 3.3. which is Oxygen pressure being 0.23 sccm, Argon was 3 sccm that has Cr<sub>2p3/2</sub> peak binding energy is more close to the Cr (III) phases. Therefore, in this section, these parameters are going to be used. Besides oxygen and argon flows rate, the way of applications for both Pulsed DC and RF Power are different. However, it can be calculated the power applied on unit of surface of the target for both techniques. The frequency of plasma is almost 100 kHz differences so that the RF Magnetron sputtering deposition is much slower than the Pulsed DC magnetron sputtering deposition is even the power applied on a unit area of surface is the same for both. Therefore, the deposition rate is also optimized for RF -Magnetron Sputtering Deposition; and it is found that the deposition 0.4-0.5 Å/sec for 40-50 W of RF Magnetron gun loaded with Pure Cr Target Materials. The rate optimized by RF power is equivalent to the deposition rate used for Pulsed DC. Furthermore, after establishing the growth parameters, the cleaning process which is employed to the sample and target in Pulsed-DC, it is also performed for RF magnetron sputtering gun's samples.

The XPS from the initial try is shown in the Figure 3.7, using the parameters mentioned above to grow Cr-Oxide. The growth of Cr-Oxide has been done for 121 Å thickness at the room temperature. During the growth process, MFC of Argon and of oxygen were fixed at 3 sccm and 0.23 sccm respectively. After getting the thickness planned, the temperature of substrate was heated up to 400°C and hold for 15 minutes and turned off annealing; the post annealing processes were done under UHV conditions. Then the sample was cooled down to RT, the sample is transferred to the analytical chamber to take XPS from its oxide surface after post annealing. XPS experiments were also repeated two times after annealing for 15 minutes at 400 °C, after one more time 500°C for 15 minutes. XPS experiments always were done at RT. The XPS result is shown in Figure 3.7. The main goal of this work was to see how the annealing effects on the Cr (III) oxide phase for RF-Magnetron Depositions. As it can be seen from the Figure 3.7 the multiple post annealing does not have any significant impact on the Cr<sub>2</sub>O<sub>3</sub> growth. It seems that XPS indicates the surface has mostly Cr<sub>2</sub>O<sub>3</sub> after annealing two times 400°C and 500°C.

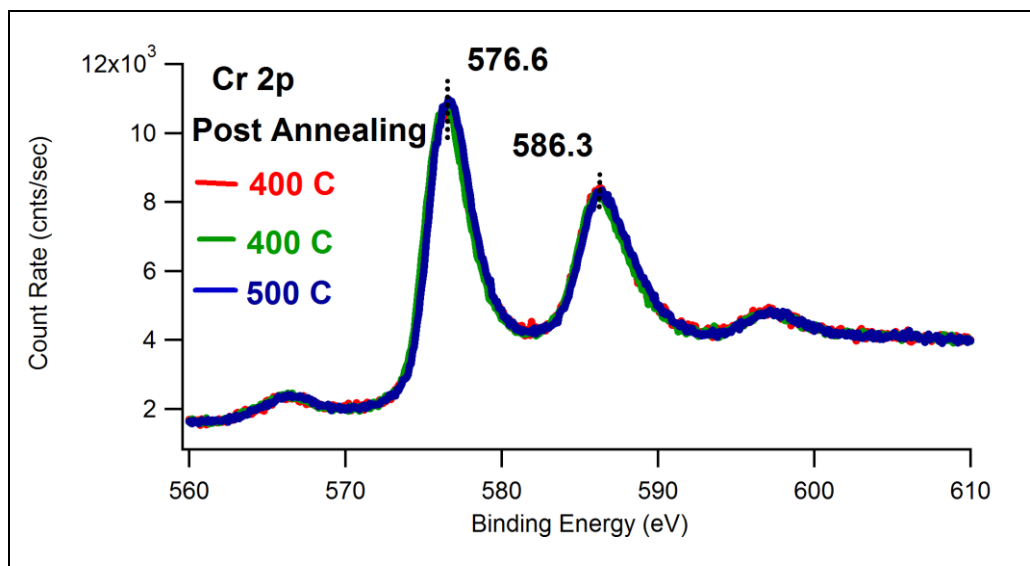


Figure 3.7: The XPS spectrum of 3 sccm Argon, 0.23 sccm Oxygen, 121 Å, substrate temperature is 400°C and post annealing has been done for 15 minutes at 400°C two times and then it again annealed at 500°C for 15 minutes for the RF1 specimen.

In the work mentioned above, which is displayed in Figure 3.7, the growth is completed in 280 seconds and the deposition rate was 0.4-0.5 Å/s. For all post annealing, the main peaks show the growth of Cr (III) phase.

In the second try, the sample was grown at 400°C (substrate temperature). And post annealing is applied after deposition. The MFC parameters were kept the same as the parameters mentioned above. This time, after the sample growth at 400°C of the substrate temperature, the post annealing has been done at 500°C for 15 minutes. The XPS results are shown in the Figure 3.8, the Cr 2p<sub>3/2</sub> peak shows on the 576.6 eV binding energy. This binding energy indicates that the Cr (III)-oxide is grown, as it is shown in the Figure 3.7. The binding energy of Cr2p<sub>3/2</sub> peak has matched with Huggins C. P. which has 576.6 eV [56]. After the sample was prepared at 400°C and the post annealing was applied at 400°C. The second and third post annealing do not show any effect on the peaks position of Cr2p<sub>3/2</sub> core orbit. It can be said that first 400°C post annealing is sufficient, the others do not need to be applied.

The XPS results coming from next work are displayed in Figure 3.8, and the sample are prepared by using the parameters the gas flow rates and applying power as the same as used before and the thickness of the thin film was also kept at the same; but in this step, the post annealing was performed at 500°C. XPS results are shown at the Figure 3.8. The thickness of Cr-oxide is 121 Å and it took 280 seconds.

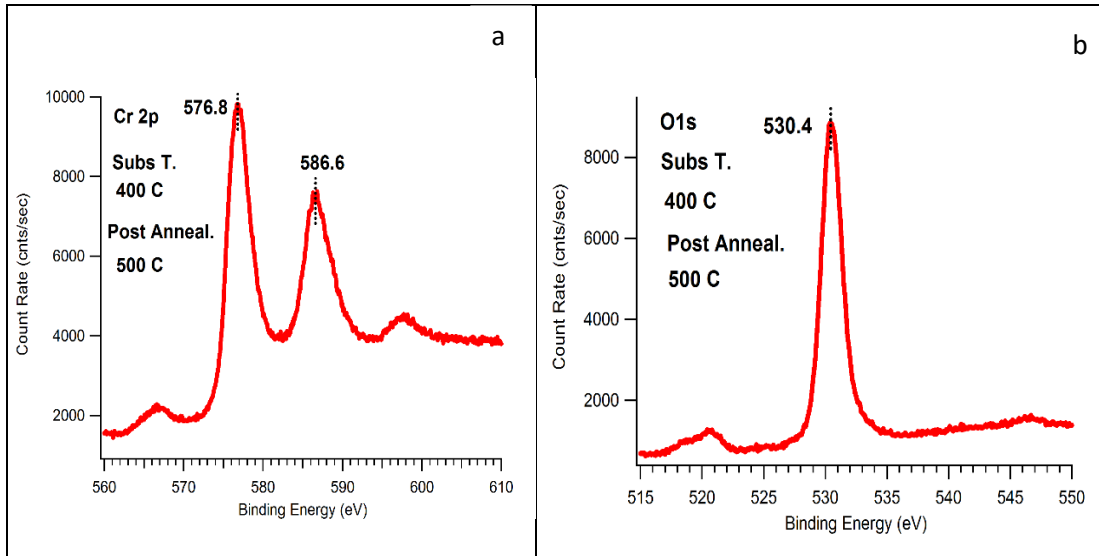


Figure 3.8: The growth of the RF2 sample has been done for 3 sccm Argon, 0.23 sccm Oxygen, 121 Å, substrate temperature is 400°C and post annealing has been done for 20 minutes at 500°C. XPS spectrum of a) Cr2p b) O1s.

The binding energy of the Cr<sub>2p<sub>3/2</sub></sub> is at 576.8 eV. This binding energy indicates that the thin film is grown as Cr<sub>2</sub>O<sub>3</sub> mostly. Another point is that the peak shape doesn't include shoulder. It can be concluded that the post annealing at 500°C succeeded to grow Cr<sub>2</sub>O<sub>3</sub> thin films. Also, the peak of O1s core orbit does not show any other feature which indicates another form of Cr-Oxide beside Cr(III)-oxide. After this achievement to ensure the growth parameter the above work is repeated as kept the parameter same. This work also shows the same result as it has been shown in Figure 3.9. While the RF2 specimen shows a very good result, which is overlapped with the literature Cr (III) [62]. By repeating the above work assures that with RF-Magnetron Sputtering system is possible to grow a chromium oxide thin film controllable. Therefore, these sample parameters need to be confirmed by repeating it.



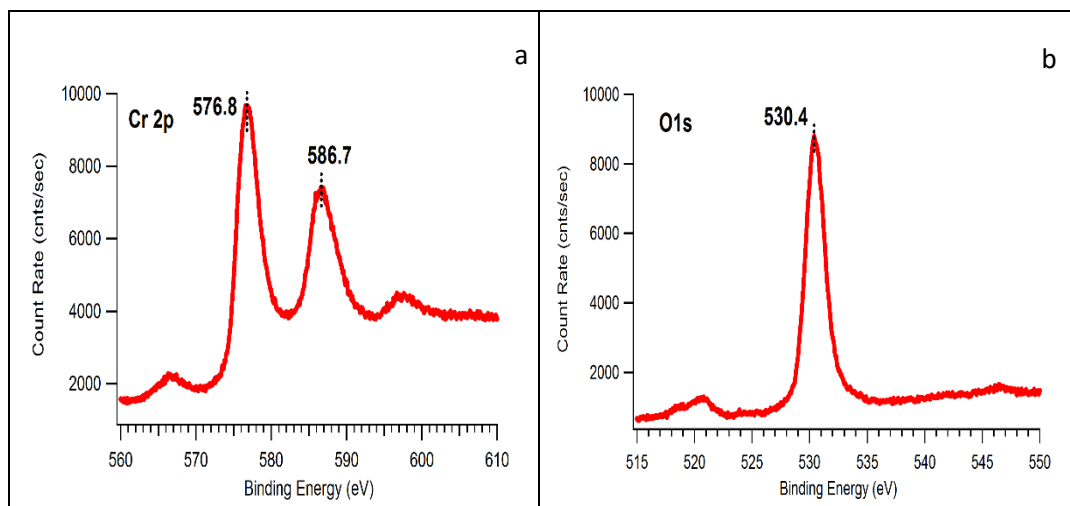


Figure 3.9: The growth has been done under 3 sccm Argon, 0.23 sccm Oxygen, 121 Å, substrate temperature is 400°C and post annealing has been done for 15 minutes at 500°C, XPS spectrum of the RF3 specimen a) Cr2p b) O1s.

After achieving the chromium oxide thin films as illustrated above, next step is concerned with growing chromium oxide thin films on silicon substrate for different parameters. The previous works have been done for RF1, RF2 and RF3 assured the substrate growth temperature, post annealing temperature and gases pressure. Mostly, growth have been done for 121 Å thickness. The following works have done little thicker than previous thin films. In this growth the thickness of the growth is less than the above work. The Cr thickness is 177 Å. During the growth the substrate temperature was 400°C and then post annealing has been done for this sample at 400°C. XPS results of Cr<sub>2p<sub>3/2</sub></sub> and O1s core peaks are shown in Figure 3.10, and the feature of peaks are the same as previous step. The thickness has been obtained for 432 seconds at 0.3-0.4 Å/s rate growth. From the spectrum the binding energy of Cr 2p<sub>3/2</sub> is 576.8 eV. This binding energy is from the Cr<sub>2</sub>O<sub>3</sub> phases.

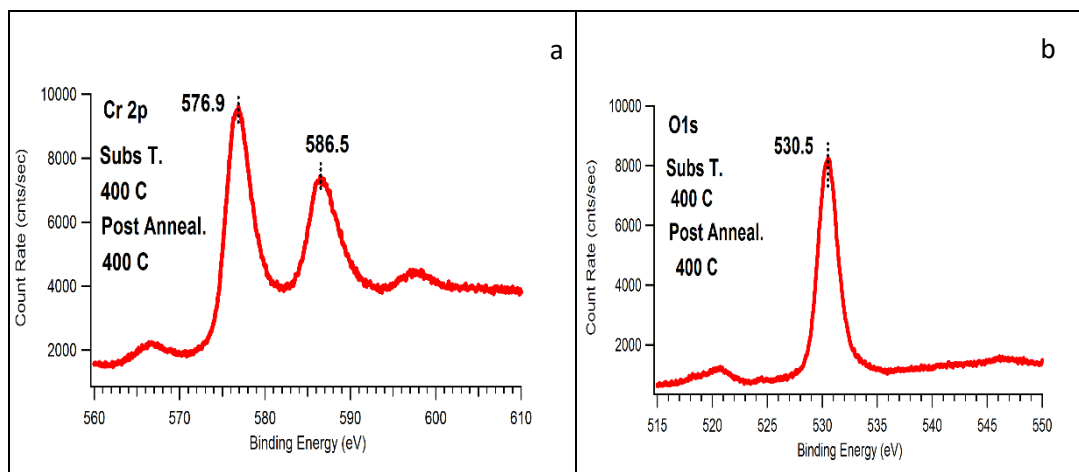


Figure 3.10: The growth of RF4 specimen has been done for 3 sccm Argon, 0.23 sccm Oxygen, 177 Å, substrate temperature is 400°C and post annealing has been done for 15 minutes at 400°C, XPS spectrum of a) Cr 2p and b) O 1s.

In the final step, the thickness was kept at 180 Å, and the growth temperature is 400°C with the same gas flow rate and RF power and the post annealing has been done at 400°C. The results of XPS for this sample are in shown in Figure 3.11.

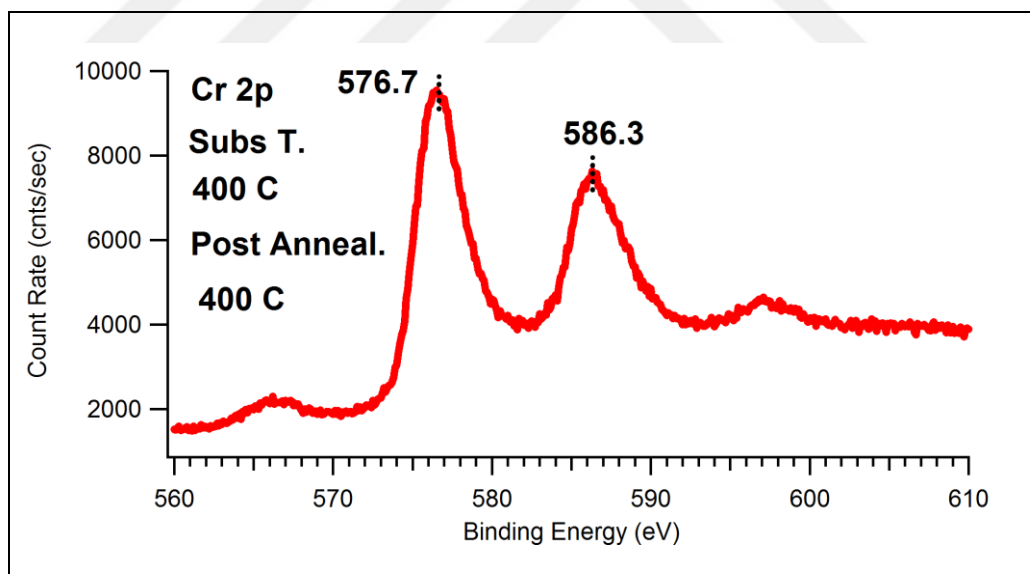


Figure 3.11: The growth has been done for 3 sccm Argon, 0.23 sccm Oxygen, 180 Å, substrate temperature is 400°C and post annealing has been done for 15 minutes at 400°C, XPS spectrum of RF5 specimen.

As it can be seen from Figure 3.11, the Cr2p<sub>3/2</sub> binding energy is 576.7 eV that is confirmed that this binding energy is related to the Cr (III). When the substrate

temperature and post annealing temperature are kept at 400°C, the samples illustrate a great Cr (III) phases.

The 400°C as growth and post annealing temperature give more successful results in order to grow thin layer of Cr<sub>2</sub>O<sub>3</sub> dominantly. Clearly, Cr(II)-oxide formation is not expected since the annealing temperature is high enough (>285°C) to decompose any formation of Cr(IV)-oxide. The Table 3.3 show possible core peak shifts of Cr2p<sub>3/2</sub> corresponding to different Cr-Oxide formations.

Table 3.3: The Photoemission peak shifts of Cr 2p<sub>3/2</sub> are shown for different Cr-Oxide formation.

Cr2p <sub>3/2</sub>	Cr (eV) <sup>0</sup>	Cr <sup>4+</sup> (eV)	Cr <sup>3+</sup> (eV)	Cr <sup>6+</sup> (eV)
References				
P. Stefanov [62]			576.7	579
H. Ma [57]	574.2		576.5	
A. Maetaki [58]	574.2	576	577	
L. Zhang [63]		576.5	577	
K Asami [61]			576	579
Huggins, C. P [56]			576.6 (±0.3)	
A. Lebugle [59]	574.26			
C. Xu [60]	574.2	576	577	

### 3.4. Fitting Process of XPS to Calculate the Cr/O Ratio

So far, it is explained how to grow Cr<sub>2</sub>O<sub>3</sub> thin films by using Magnetron Sputtering Deposition techniques and the growth parameters optimized are tabulated above. The Chromium Oxide thin films have been grown on the naturally oxidized on Si (100) crystal and discussed each of the step changes changing the growth parameters. As it is well known that ultra-thin films are not easy to be characterized their phases structurally by using bulk techniques such as XRD, SEM so on... The best technique to analyzing their oxide phase is surface electron photoemission

experiment since it has surface sensitivity and it can deliver the information of chemical, structural, and electronic properties within atomic sensitivity. In this study, XPS is only used to search oxidation phases of Cr-Oxide surfaces.

The growths have been succeeded as they were described previous sections, the results of XPS were illustrated to show how the growth parameters affect to oxidation phases in ultra-thin films. The main target is to success the growth of  $\text{Cr}_2\text{O}_3$  surface since it is a nominated perfect antiferromagnetic layer in the spintronic devices built by multilayer thin films. As it is well known that  $\text{Cr}_2\text{O}_3$  films has a distinct satellite feature in the photoemission spectrums of  $\text{Cr}2p_{3/2}$ ; and it helps to assure to grow the perfect  $\text{Cr}_2\text{O}_3$  surface. Nevertheless, the analyses of photoemission spectrum are necessary for a tedious fitting process. It provides the elemental ratios with the chemical and electronic structure. In this study, the program CASA (product of SPECS GmbH) is used to analyze the results of XPS.

The success of fitting process in XPS analyzes depends on the good background functions such as Shirley and Taggard functions and on the function illustrated the core peaks of  $\text{Cr}2p_{3/2}$ ,  $\text{O}1s$ , and the satellite peaks of  $\text{Cr(III)}$ . Figure 3.12 shows a survey containing the XPS from four sample growth. The sample Si (100) is a XPS survey taken from the substrate, and it shows only Silicon and Oxygen Core peaks with Auger features. It indicates that the substrate is clean enough and ready to grow Cr-oxide films. There are other observations on the survey spectrums of Cr-Oxide films that any of Si features do not present since the thickness of oxide films buried the photoemission peaks coming from the substrate. Meanwhile, the four surveys indicate in first overview that all films show Cr-Oxide surfaces but it is not easy to say which one is perfect  $\text{Cr}_2\text{O}_3$  surface. That's why the windows for the core orbit  $\text{Cr}2p_{3/2}$  and  $\text{O}1s$  were taken for every four samples.

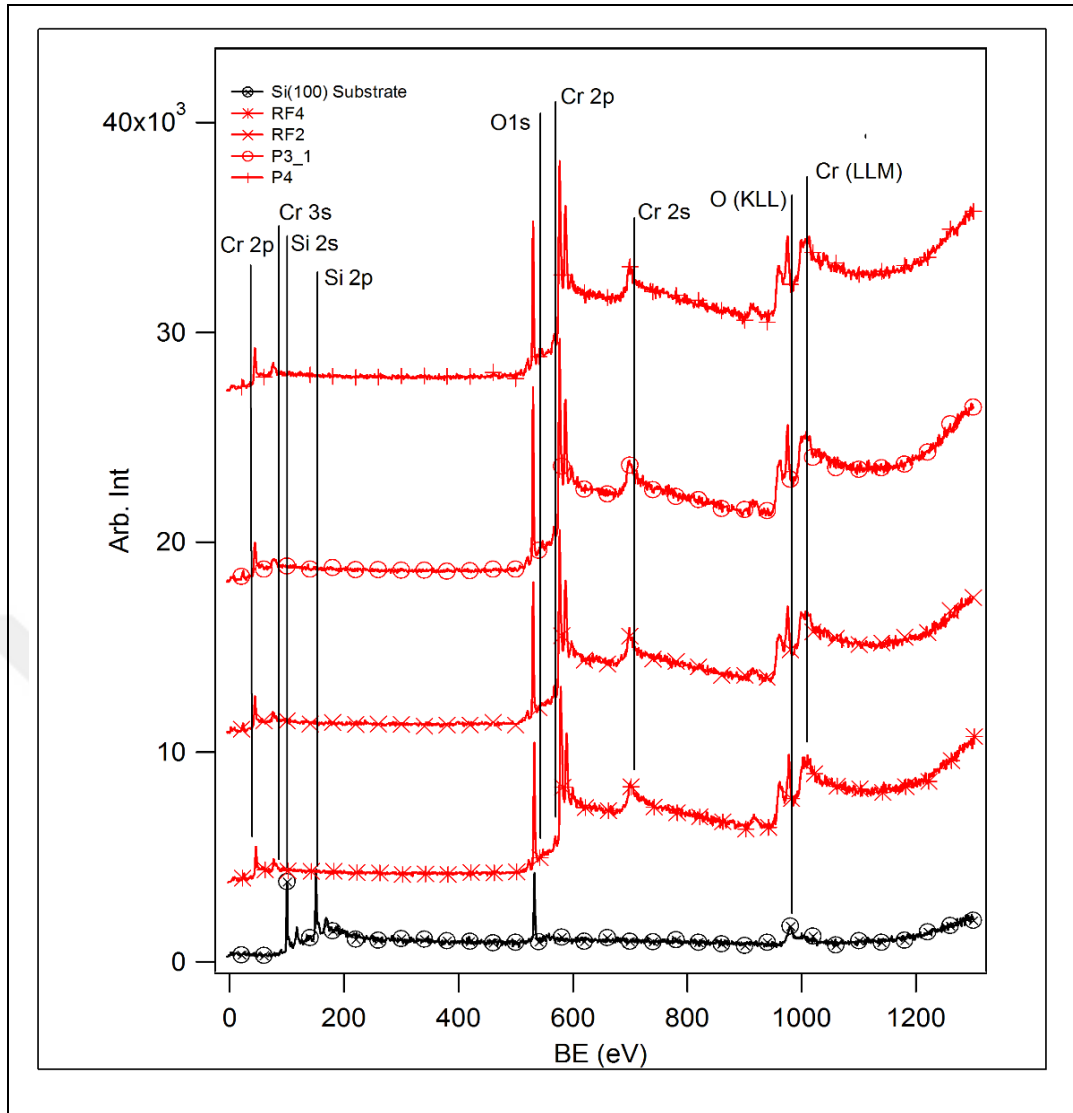


Figure 3.12: The survey spectrum of Cr-Oxide surfaces and natural oxidized Si (100) crystal.

All XPS windows of Cr2p and O1s show almost same feature, but there is a small difference that can be prove by fitting study. Therefore, the photoemission spectrums of Cr2p and O1s were taken with higher energy resolution, and the subtraction of Shirley background function were applied for all spectrums, then by using Voigt function, the peaks of Cr2p and O1s were analyzed to reveal the number of possible peak and energy shift with the function of the calculated peak area. Figure 3.13 shows fitting process done for Cr2p and O1s of the sample RF2.

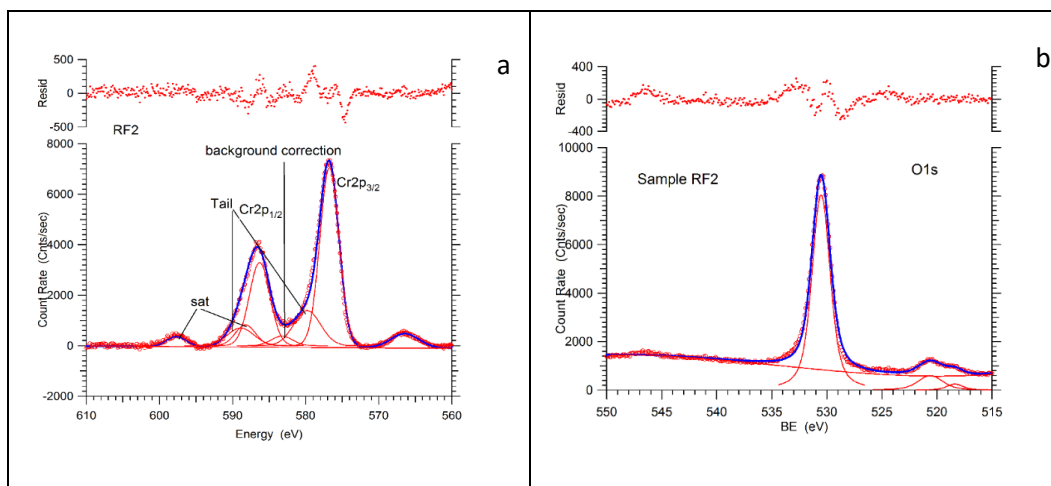


Figure 3.13: Fitting process of a) Cr2p and b) O1s.

The O1s does not indicate any other oxygen correlation and also the peak position is appropriate with Cr(III). However, the photoemission peak of Cr2p is more complex than O1s. The main peak comes from Cr(III) but there are tails on Cr2p<sub>3/2</sub> and Cr<sub>1/2</sub> clearly due to the electronic structure of valance band for transition metal oxide. Other than tails, the satellite feature also were observed on spectrum, and it indicates clearly Cr (III) oxide formations. However, there is a possibility for the existence Cr (VI) with same binding energy shift from metallic Cr (0). If there is Cr (VI), it should have trace amount. In order to prove existence of optimum Cr (III)-oxide films, the ratio between the area of Cr2p and O1s should be calculated; as long as the ratio of calculated area is closest to 2/3, the surface is close to Cr(III)-oxide formation. The calculated atomic ratio is tabulated in Table 3.4. According to the calculated peak area treated with Atomic sensitivity of Cr2p and O1s, RF2 is the most Cr (III)-Oxide sample.

Table 3.4: The calculation of the four samples Cr/O ratios.

Samples	Power (W)	Post Anneal. (°C)	Growth Temp. (°C)	Gas Flow Rate		Thick. (Å)	Atomic Ratio Cr/O
				Argon SCCM	Oxygen SCCM		
RF2	RF 20	500	400	3.0	0.23	121	40/60
RF4	RF 20	400	400	3.0	0.23	177	42.44/57.56
P3_1	DC 25	RT	250	3.0	0.23	114	40/60
P4	DC 25	400	400	3.0	0.23	99	41.76/58.24

### 3.5. Discussion

As it was discussed aforementioned, the Cr oxides, grown with Pulsed DC and RF magnetron sputtering, have difficulties that limit the growth process. Pulsed DC relatively is mostly faster than the RF spectrum. It is observed that in order to deposit metal oxide films, the deposition rate of Pulsed DC is higher than the RF. The RF can have same Cr coating ratio at high voltage compare to the Pulsed DC. Although the Pulsed DC have high deposition ratio, it is poisoned for long period reactive depositions because the metallic target exposed to the oxygen and it is oxidized in time; while oxygen is fed to the system to make thin  $\text{Cr}_x\text{O}_y$  film on Si crystal substrate.

Another important point is that the substrate temperature effects on growth process. Both the temperature used for the substrate and post annealing have effect on  $\text{Cr}^{3+}$  phase's growth. While growing Cr oxide on Si crystal at low temperatures ( $\sim 100^\circ\text{C}$ ), the  $\text{Cr}^{4+}$  phases occur. After applied post annealing above  $250^\circ\text{C}$ , the  $\text{Cr}^{4+}$  decomposes to the  $\text{Cr}^{3+}$  as it displayed in Figure 3.4.

Nevertheless, the parameters optimized for Pulsed-DC Magnetron sputtering deposition process do not work as well for RF Magnetron sputtering. For comparable work, some of parameters were used as same as used for Pulsed DC; such as the gases pressure. However, the power applied on unit of surface are optimized to have same

deposition ratio. Then the temperature of the substrate and post annealing have been seeking in order to make the most Cr(III)-oxide surface.

Finally, the thin Cr<sub>2</sub>O<sub>3</sub> film has been achieved with optimized parameter by both Pulsed DC and RF on naturally oxidized silicon crystal (100) reproducibly. It is concluded that the RF-Magnetron Sputtering deposition technology is the best optimized technique to make metal oxide surface reproducibly. The advantage is that the parameter optimized experimentally may be easily modeled for industrial applications such as spintronic devices having the multilayer film structure which the Cr<sub>2</sub>O<sub>3</sub> can be used as antiferromagnetic ultra-thin layer.





## 4. CONCLUSION

Chromium oxides, as transition metal oxide thin films have wide technological applications such as a layer having strong magnetic moment enhancement in multilayers films as single layer form exhibiting ferromagnetic or antiferromagnetic properties and some oxide formations showing high coercivity towards spintronic devices. Nevertheless, Chromium has also variety oxide phases like  $\alpha$ -Cr<sub>2</sub>O<sub>3</sub>,  $\gamma$ -Cr<sub>2</sub>O<sub>3</sub>, CrO<sub>2</sub>, CrO<sub>3</sub>, Cr<sub>8</sub>O<sub>21</sub>, Cr<sub>2</sub>O<sub>5</sub>, and, Cr<sub>3</sub>O<sub>4</sub>, and this creates great opportunity to be used in many applications but it also creates difficulties during fabrication. The form of oxidations is strictly depended on the way of fabrications. So far, chromium oxide films are also used many times as bulk or films formations but not as in angstrom ranges. When the growth range goes under the Nano Range, it exhibits that the ultra-thin films of Chromium oxide get easily multi phases; it is not easy to grow single oxide phase even though reproducibly.

In this study, the selected chromium oxide phase is Cr<sub>2</sub>O<sub>3</sub>, which is the most stable one, was grown as in ultra-thin film by using Magnetron Sputtering Deposition Technique; the films grown were analyzed by the surface photoemission spectroscopy XPS, one is strong surface analyzing technique. The growth and analyzing processes were done in UHV conditions and the sample prepared were never introduced in atmospheric conditions; Once the substrate Si (100) naturally oxidized are loaded after preparing UHV conditions. Cr<sup>+3</sup>-Oxide phase is the most stable one of them but it would easily contain the other oxide formation base on the ratio of oxygen in growth conditions, annealing temperature and grain size coming off from the magnetron target.

The magnetron sputtering (MS) deposition would be executed by DC, Pulsed DC, and RF power sources in reactive growth condition with the certain ratios of Argon and Oxygen. Meanwhile, the substrates would be heated during growth (annealing) and after growth process (post annealing), Chromium particles coming from the target of MS is oxidized even before hitting on the substrate. Contrary, the way of applying power in order to generate plasma has serious effects wearing the target. DC Power technique used with the reactive plasma is poisoning target in short time. In the Pulsed DC, the target poisoning by molecular oxygen in reactive plasma become slowly with the function of applying power but it is not good for controlled

manner deposition. On the other hand, RF has good timing with his unique frequency interval in order to clean poisoned surface in short time. Therefore, it has always stable deposition but slow since in the half of time, the plasma cleans the surface from charging occurring because of the thin layer on oxide target surface. The other advantage is to have the small size particles coming off the target.

The size of particles should be well distributed and they should be as possible as smaller. It is important to oxide particles completely on the surface homogenously. The size is not the only important thing for fully oxidation; the temperature is also important. While continuing annealing after deposition, the structure of oxide surface alters in grain size and electronic structure resulting to different oxide level. In MS Deposition Technique, the power applied on the surface of target causes changing the size of particles coming from the target, and the size of particles also effect oxide level as the ratio of oxygen in mixed process gas during acting plasma does. Therefore, if considering reproducible growth with single phase, the particle size depending on the applied power, annealing-post annealing temperatures and gas ratio of Argon and oxygen during acting plasma should be optimized substantially. On the other hand, the sensitivity of characterization also is essential to trace optimized parameter to grow the most stable single phase oxide surface.

In this study, many samples were prepared but just four sample were presented since they have only meaningful spectroscopic results.  $\text{Cr}^{+3}$ -Oxide has distinct two features in the widow of Cr2p x-ray photoemission spectroscopy, and it is used to characterize  $\text{Cr}_2\text{O}_3$  surface. At the same time, the window of O1s should show one type of oxidation while not showing the other oxide peak by shifting. However, this is not enough to prove having fully  $\text{Cr}_2\text{O}_3$  surface. The atomic ratio of Cr/O should be 2/3. That's why the peak areas of Cr2p and O1s were found out by using appropriate peak and background functions with ASF in order to calculate atomic ratios. The only one sample called by RF2 has 2/3 atomic rate, but it is not enough that the surface has a single oxide phase. It is known that  $\text{Cr}_2\text{O}_3$  has  $\alpha$  and  $\gamma$  phases which have different symmetries but have same electronic structure. That's why it is necessary to crystallographic study. However, the thickness of oxide layer is enough to allow XRD but XPD, STM and LEED. Next level, the oxide surface with optimized parameters should be worked by XPD, STM and LEED to define structural feature with electronic structure. That's why it is planed that Cr-Oxide with two  $\alpha$ - and  $\gamma$ - $\text{Cr}_2\text{O}_3$  two phases will be studied epitaxial in order to define the structural differences.

## REFERENCES

- [1] Schwarz K., (1986), "CrO<sub>2</sub> predicted as a half-metallic ferromagnet", *Journal of Physics F: Metal Physics*, 16(9), L211.
- [2] Ivanov P. G., Bussmann K. M., (2009), "Temperature stability of the half-metallic CrO<sub>2</sub> (110) and (001) surfaces in ultrahigh vacuum", *Journal of Applied Physics*, 105(7), 7B107.
- [3] Kämper K. P., Schmitt W., Güntherodt G., Gambino R. J., Ruf R., (1987), "CrO<sub>2</sub>—A New Half-Metallic Ferromagnet", *Physical review letters*, 59(24), 2788.
- [4] Dedkov Y. S., Vinogradov A. S., Fonin M., König C., Vyalikh D. V., Preobrajenski A. B., Molodtsov S. L., (2005), "Correlations in the electronic structure of half-metallic ferromagnetic CrO<sub>2</sub> films: An x-ray absorption and resonant photoemission spectroscopy study", *Physical Review B*, 72(6), 060401.
- [5] Robbert P. S., Geisler H., Ventrice Jr C. A., Van Ek J., Chaturvedi S., Rodriguez J. A., Diebold U., (1998), "Novel electronic and magnetic properties of ultrathin chromium oxide films grown on Pt (111)", *Journal of Vacuum Science & Technology A*, 16(3), 990-995.
- [6] Priyantha W. A. A., Waddill G. D., (2005), "Structure of chromium oxide ultrathin films on Ag (111)", *Surface science*, 578(1), 149-161.
- [7] Demirci E., Öztürk M., Öcal M. T., Öztürk O., Akdoğan N., (2015), "Investigation of spin canting phenomena in perpendicularly exchange biased Pt/Co/Pt/Cr<sub>2</sub>O<sub>3</sub> thin films", *Thin Solid Films*, 591, 72-75.
- [8] Lim S. H., Murakami M., Lofland S. E., Zambano A. J., Salamanca-Riba L. G., Takeuchi I., (2009), "Exchange bias in thin-film (Co/Pt)<sub>3</sub>/Cr<sub>2</sub>O<sub>3</sub> multilayers", *Journal of Magnetism and Magnetic Materials*, 321(13), 1955-1958.
- [9] Cheng C. S., Gomi H., Sakata H. (1996), "Electrical and optical properties of Cr<sub>2</sub>O<sub>3</sub> films prepared by chemical vapour deposition", *physica status solidi (a)*, 155(2), 417-425.
- [10] Ivanov P. G., Watts S. M., Lind D. M., (2001), "Epitaxial growth of CrO<sub>2</sub> thin films by chemical-vapor deposition from a Cr<sub>8</sub>O<sub>21</sub> precursor", *Journal of Applied Physics*, 89(2), 1035-1040.
- [11] Rabe M., Dreßen J., Dahmen D., Pommer J., Stahl H., Rüdiger U., Hesse D., (2000), "Preparation and characterization of thin ferromagnetic CrO<sub>2</sub> films for applications in magnetoelectronics", *Journal of magnetism and magnetic materials*, 211(1), 314-319.

- [12] Finger L. W., Hazen, R. M., (1980), "Crystal structure and isothermal compression of  $\text{Fe}_2\text{O}_3$ ,  $\text{Cr}_2\text{O}_3$ , and  $\text{V}_2\text{O}_3$  to 50 kbars", *Journal of Applied Physics*, 51(10), 5362-5367.
- [13] Sokolov A., Yang C. S., Yuan L., Liou S., Cheng R., Xu B., Doudin, B., (2002), "Spin blockade effects in chromium oxide intergrain magnetoresistance.", *Journal of Applied Physics* 91 8801-8803.
- [14] Monnereau O., Tortet L., Grigorescu C. E. A., Savastru D., Iordanescu C. R., Guinneton F., Stanoi D., (2010), "Chromium oxides mixtures in PLD films investigated by Raman spectroscopy", *Journal of Optoelectronics and Advanced Materials*, 12(8), 1752.
- [15] Soulen R. J., Byers J. M., Osofsky M. S., Nadgorny B., Ambrose T., Cheng S. F., Barry A., (1998), "Measuring the spin polarization of a metal with a superconducting point contact", *science*, 282(5386), 85-88.
- [16] Sahoo S., Binek C., (2007), "Piezomagnetism in epitaxial  $\text{Cr}_2\text{O}_3$  thin films and spintronic applications", *Philosophical Magazine Letters*, 87(3-4), 259-268.
- [17] Foner S., (1963), "High-field antiferromagnetic resonance in  $\text{Cr}_2\text{O}_3$ ", *Physical Review*, 130(1), 183.
- [18] De Rossi A., Conti C., Trillo S., (1998), "Stability, multistability, and wobbling of optical gap solitons", *Physical review letters*, 81(1), 85.
- [19] Ku R. C., Winterbottom W. L., (1985), "Electrical conductivity in sputter-deposited chromium oxide coatings", *Thin Solid Films*, 127(3-4), 241-256.
- [20] Pradier C. M., Rodrigues F., Marcus P., Landau M. V., Kaliya M. L., Gutman A., Herskowitz M., (2000), "Supported chromia catalysts for oxidation of organic compounds: the state of chromia phase and catalytic performance", *Applied Catalysis B: Environmental*, 27(2), 73-85.
- [21] Rajesh H., Ozkan U. S., (1993), "Complete oxidation of ethanol, acetaldehyde and ethanol/methanol mixtures over copper oxide and copper-chromium oxide catalysts", *Industrial & engineering chemistry research*, 32(8), 1622-1630.
- [22] Dai J., Tang J., Xu H., Spinu L., Wang W., Wang K., Diebold U., (2000), "Characterization of the natural barriers of intergranular tunnel junctions:  $\text{Cr}_2\text{O}_3$  surface layers on  $\text{CrO}_2$  nanoparticles", *Applied Physics Letters*, 77(18), 2840-2842.
- [23] Weckhuysen B. M., Schoonheydt R. A., (1999), "Alkane dehydrogenation over supported chromium oxide catalysts", *Catalysis Today*, 51(2), 223-232.

- [24] Ranno L., Barry A., Coey J. M. D., (1997), "Production and magnetotransport properties of CrO<sub>2</sub> films", *Journal of applied physics*, 81, 5774-5776.
- [25] Kubota B., (1961), "Decomposition of higher oxides of chromium under various pressures of oxygen", *Journal of the American Ceramic Society*, 44(5), 239-248.
- [26] Shibasaki Y., Kanamaru F., Koizumi M., Kume S., (1973), "CrO<sub>2</sub>-Cr<sub>2</sub>O<sub>3</sub> Phase Boundary Under High O<sub>2</sub> Pressures", *Journal of the American Ceramic Society*, 56(5), 248-249.
- [27] Ivanov P. G., Watts S. M., Lind D. M., (2001), "Epitaxial growth of CrO<sub>2</sub> thin films by chemical-vapor deposition from a Cr<sub>8</sub>O<sub>21</sub> precursor", *Journal of Applied Physics*, 89(2), 1035-1040.
- [28] Stanoi D., Socol G., Grigorescu C., Guinneton F., Monnereau O., Tortet L., Mihailescu I. N., (2005), "Chromium oxides thin films prepared and coated in situ with gold by pulsed laser deposition", *Materials Science and Engineering: B*, 118(1), 74-78.
- [29] Aguilera C., González J. C., Borrás A., Margineda D., González J. M., González-Elipé A. R., Espinós, J. P., (2013), "Preparation and characterization of CrO<sub>2</sub> films by Low Pressure Chemical Vapor Deposition from CrO<sub>3</sub>", *Thin Solid Films*, 539, 1-11.
- [30] Zhang X., Zhong X., Visscher P. B., LeClair P. R., Gupta A., (2013), "Structural and magnetic properties of epitaxial CrO<sub>2</sub> thin films grown on TiO<sub>2</sub> (001) substrates", *Applied Physics Letters*, 102(16), 162410.
- [31] Maddox B. R., Yoo C. S., Kasinathan D., Pickett W. E., Scalettar, R. T., (2006), "High-pressure structure of half-metallic CrO<sub>2</sub>", *Physical Review B*, 73(14), 144111.
- [32] Cho Y. N., DeSisto W. J., (2003), "Phase-Selective CVD of Chromium Oxides from Chromyl Chloride", *Chemical Vapor Deposition*, 9(3), 121-124.
- [33] Barry A., Coey J. M. D., Viret, M., (2000), "A CrO<sub>2</sub>-based magnetic tunnel junction", *Journal of Physics: Condensed Matter*, 12(8), L173.
- [34] Lubitz P., Rubinstein M., Osofsky M. S., Nadgorny B. E., Soulen R. J., Bussmann K. M., Gupta A., (2001), "Ferromagnetic resonance observation of exchange and relaxation effects in CrO<sub>2</sub>", *Journal of Applied Physics*, 89(11), 6695-6697.
- [35] Leo T., Kaiser C., Yang H., Parkin S. S., Sperlich M., Güntherodt G., Smith, D. J., (2007), "Sign of tunneling magnetoresistance in CrO<sub>2</sub>-based magnetic tunnel junctions", *Applied Physics Letters*, 91(25), 252506.

- [36] Hones P., Diserens M., Levy F., (1999), "Characterization of sputter-deposited chromium oxide thin films", *Surface and Coatings Technology*, 120, 277-283.
- [37] Arca E., Fleischer K., Krasnikov S. A., Shvets I., (2013), "Effect of chemical precursors on the optical and electrical properties of p-type transparent conducting Cr<sub>2</sub>O<sub>3</sub>: (Mg, N)", *The Journal of Physical Chemistry C*, 117(42), 21901-21907.
- [38] Abu-Shgair K., Abu-Safe H. H., Aryasomayajula A., Beake B., Gordon M. H., (2010), "Characterizing crystalline chromium oxide thin film growth parameters", *Reviews on Advanced Materials Science*, 24, 64-68.
- [39] Contoux G., Cosset F., Celerier A., Machet J., (1997), "Deposition process study of chromium oxide thin films obtained by dc magnetron sputtering", *Thin Solid Films*, 292(1), 75-84.
- [40] Watts J. F., Wolstenholme J., (2003), "An introduction to surface analysis by XPS and AES", Wiley-VCH.
- [41] Honig R. E., (1976), "Surface and thin film analysis of semiconductor materials", *Thin Solid Films*, 31(1), 89-122.
- [42] Granqvist C. G., (2012), "Preparation of thin films and nanostructured coatings for clean tech applications: A primer", *Solar Energy Materials and Solar Cells*, 99, 166-175.
- [43] Kelly P. J., Arnell R. D., (2000), "Magnetron sputtering: a review of recent developments and applications", *Vacuum*, 56(3), 159-172.
- [44] Bräuer G., Szyszka B., Vergöhl M., Bandorf R., (2010), "Magnetron sputtering—Milestones of 30 years", *Vacuum*, 84(12), 1354-1359.
- [45] Mientus R., Grötschel R., Ellmer K., (2005), "Optical and electronic properties of CrO<sub>x</sub>N<sub>y</sub> films, deposited by reactive DC magnetron sputtering in Ar/N<sub>2</sub>/O<sub>2</sub>(N<sub>2</sub>O) atmospheres", *Surface and Coatings Technology*, 200(1), 341-345.
- [46] Hollander J. M., Jolly W. L., (1970). "X-ray photoelectron spectroscopy", *Accounts of chemical research*, 3(6), 193-200.
- [47] Tipler P. A., Llewellyn R. A., (2008), "Modern physics", 5<sup>th</sup> Edition, Freeman.
- [48] Chusuei C. C., Goodman D. W., (2002), "X-ray photoelectron spectroscopy", *Encyclopedia of physical science and technology*, 17, 921-938.
- [49] Somorjai G. A., (1981), "Chemistry in two dimensions: surfaces", Cornell University Press, Ithaca.

- [50] Seah M. P., Dench W. A., (1979), "Quantitative electron spectroscopy of surfaces: a standard data base for electron inelastic mean free paths in solids", *Surface and interface analysis*, 1(1), 2-11.
- [51] Fulghum J. E., (1999), "Recent developments in high energy and spatial resolution analysis of polymers by XPS", *Journal of electron spectroscopy and related phenomena*, 100(1), 331-355.
- [52] Liu F., Li J., Li Q., Wang Y., Zhao X., Hua Y., Liu X., (2014), "High pressure synthesis, structure, and multiferroic properties of two perovskite compounds  $Y_2FeMnO_6$  and  $Y_2CrMnO_6$ ", *Dalton Transactions*, 43(4), 1691-1698.
- [53] Biesinger M. C., Lau L. W., Gerson A. R., Smart R. S. C., (2010), "Resolving surface chemical states in XPS analysis of first row transition metals, oxides and hydroxides: Sc, Ti, V, Cu and Zn", *Applied Surface Science*, 257(3), 887-898.
- [54] Aronniemi M., Sainio J., Lahtinen J., (2005), "Chemical state quantification of iron and chromium oxides using XPS: the effect of the background subtraction method", *Surface science*, 578(1), 108-123.
- [55] Hesse R., Streubel P., Szargan R., (2007), "Product or sum: comparative tests of Voigt, and product or sum of Gaussian and Lorentzian functions in the fitting of synthetic Voigt-based X-ray photoelectron spectra", *Surface and Interface Analysis*, 39(5), 381-391.
- [56] Huggins C. P., Nix R. M., (2005), "Growth and characterisation of  $Cr_2O_3$  (0001) thin films on Cu (111)", *Surface science*, 594(1), 163-173.
- [57] Ma H., Berthier Y., Marcus P., (1999), "AES, XPS, and TDS study of the adsorption and desorption of  $NH_3$  on ultra-thin chromium oxide films formed on chromium single crystal surfaces", *Applied surface science*, 153(1), 40-46.
- [58] Maetaki A., Kishi, K., (1998), "Preparation of ultrathin chromium oxide films on Cu (110) investigated by XPS and LEED", *Surface science*, 411(1), 35-45.
- [59] Lebugle A., Axelsson U., Nyholm R., Mårtensson N., (1981), "Experimental L and M core level binding energies for the metals  $^{22}Ti$  to  $^{30}Zn$ ", *Physica Scripta*, 23(5A), 825.
- [60] Xu C., Hassel M., Kuhlenbeck H., Freund, H. J., (1991), "Adsorption and reaction on oxide surfaces:  $NO$ ,  $NO_2$  on  $Cr_2O_3$  (111)/Cr (110)", *Surface science*, 258(1), 23-34.
- [61] Asami K., Hashimoto K., (1977), "The X-ray photo-electron spectra of several oxides of iron and chromium", *Corrosion Science*, 17(7), 559-570.

- [62] Stefanov P., Stoychev D., Stoycheva M., Marinova T., (2000), "XPS and SEM studies of chromium oxide films chemically formed on stainless steel 316 L", *Materials Chemistry and Physics*, 65(2), 212-215.
- [63] Zhang L., Kuhn M., Diebold U., (1997), "Growth, structure and thermal properties of chromium oxide films on Pt (111)", *Surface science*, 375(1), 1-12.





## **BIOGRAPHY**

İsmet Gelen was Born at 1986, in Bingöl, Turkey. He went Elementary School in Bingöl. He went High School in İstanbul and graduated at 2006. He started in physics at Gebze Institute of Technology (GIT) in 2006. He got bachelor's degree from Gebze Institute of Technology at 2011 in Physics. He started master degree at the same university. However, he went to USA to obtain his master degree from Georgia State University at 2015 in Physics.



## APPENDICES

“The Growth of Chromium Oxide Thin Films by Reactive Magnetron Sputtering Deposition” s.22 Melek TÜRKSOY ÖCAL, İsmet GELEN, Baha Sakar, Sibel TOKDEMİR ÖZTÜRK, Osman ÖZTÜRK Fizik ABD, GTU FEN BİLİMLERİ LİSANSÜSTÜ ARAŞTIRMALAR SEMPOZYUMU & TANITIM GÜNLERİ 2016

